Reversible phosphorylation of WOX5 protein controls the homeostasis of QC

Ling Chen[1*]

[1]State Key Laboratory of Hybrid Rice, Institute of Advanced Studies. Wuhan University, WuHan, China

[*]corresponding author: lingchen0206@whu.edu.cn

Highlights

The subfamily II of AtSKs stabilizes WOX5 protein by phosphorylating the GSK3 Motifs in the PEST domain

The subfamily II of the catalytic subunit of AtPP2A-Cs holoenzymes destabilizes WOX5 protein by dephosphorylating GSK3 Motifs

Reversible phosphorylation of WOX5 protein controls the homeostasis of the low proliferative activity of the QC cells and of the constant one-layer QC

In situ overexpressed WOX5 protein and phosphate-mimicked WOX5 protein are both sufficient for producing more quiescent cells

Summary

Fundamental questions of structural and functional homeostasis of the *Arabidopsis* QC in root stem cell niche remain elusive. WUSCHEL-RELATED HOMEOBOX 5 (WOX5) protein, which serves as a QC marker, yet the regulation of its homeostasis remains unknown. Here, we characterize a novel role of PEST domain in WOX5 protein, which stabilizes WOX5 protein by phosphorylating GSK3 Motifs (GMs). Next, we demonstrate that the subfamily II of *Arabidopsis* SHAGGY-like Kinases (AtSKs) stabilizes WOX5 protein by phosphorylating the GMs in the PEST domain and the subfamily II of the catalytic subunit of *Arabidopsis* PP2A (AtPP2A-Cs) holoenzymes destabilizes WOX5 protein by dephosphorylating the GMs. Moreover, we find both in situ overexpressed and phosphate-mimicked WOX5 protein can reduce the proliferative activity of the original stele initials (SI) and its daughter cells (SID), leading to the production of more quiescent cells. Taken together, our findings suggest that the homeostasis of WOX5 protein is modulated by reversible phosphorylation, which functionally controls the homeostasis of the QC cells' low proliferative activity. Furthermore, the subfamily II of AtPP2A-Cs structurally controls the homeostasis of one-layer QC by down-regulating WOX5 expression and destabilizing WOX5 protein in the SI and SID.

Introduction

The quiescent centre (QC) was discovered and named by Frederick Albert Lionel Clowes through observations of root tips of numerous plant species. Its existence was validated through the use of X-irradiation and radioisotopes tracing in the 1950s (Barlow, 2015a, b; Barlow, 2015c; Dubrovsky and Barlow, 2015). Clowes's subsequent work confirmed that the QC mainly consists of G1 cells, which were not in a strictly quiescent state but in a resting state that can slowly participate in the cell cycle when needed (Clowes, 1968). Until 1993, the QC of *Arabidopsis thaliana* was firstly described by Dolan and his colleagues (Dolan et al., 1993). Thus, the definition of QC in *Arabidopsis* includes two aspects: Structurally, the QC, which is one layer cells (average of four cells) reside at the center of the "closed root apical meristem (RAM)", surrounded by initials (Clowes, 1981; Dolan et al., 1993); Functionally, these one-layer QC cells with a very low rate of nuclear DNA synthesis or very low proliferative activity serve as a reservoir of surrounding mitotically active stem cells and the organizer of the stem cell niche (SCN) (Barlow, 2015c; Claudia et al., 1997; Dubrovsky and Barlow, 2015).

To date, great progress in molecular regulation of *Arabidopsis* QC's formation and function has been made. Two GRAS family transcription factors SCARECROW (SCR) and SHORT-ROOT (SHR) play a prominent role in positioning and specifying the QC. They form a ternary complex with RETINOBLASTOMA-RELATED (RBR) to inhibit asymmetric stem cell division and reinforce quiescence in the QC (Cruz-Ramírez et al., 2012; Cruz-Ramírez et al., 2013; Laurenzio et al., 1996; Nakajima et al., 2001; Sabatini et al., 2003). Additionally, the C2H2 zinc finger family transcription factor JACKDAW (JKD) (one of the BIRDs) contributes to QC specification and maintenance by interacting with SCR and SHR (Clark et al., 2020; Long et al., 2015; Long et al., 2017). Similarly, PLETHORA (PLT) family of AP2-domain transcription factors are required for the QC specification and maintenance. These factors operate in a parallel pathway with SCR and SHR or in a convergence path with SCR through forming a ternary complex with teosinte-branched cycloidea PCNA (TCP) transcription factors (Aida et al., 2004; Shimotohno et al., 2018). However, why the QC cells always occupy just one layer area or constantly exist just one layer at the centre of RAM in *Arabidopsis* remains elusive.

Many factors modulate the proliferative activity of QC cells in *Arabidopsis*. One such factor is the CELL CYCLE SWITCH 52 A (CCS52A), which mediates the repression of the QC's proliferative activity in by activating the anaphase promoting complex/cyclosome (APC/C) (Vanstraelen et al., 2009). Another factor, the ethylene response factor 115 (ERF115), is a target

of the complex of APC/C^{CCS52A2} E3 ubiquitin ligase. ERF115 is naturally inhibited by proteolysis, and promotes QC cells proliferation by activating the phytosulfokine 5 (PSK5) peptide in response to brassinosteroid or damage to the root (Jefri et al., 2013). ASH1-RELATED3 (ASHR3), a histone 3 lysine methyltransferase, is a direct target of E2Fa/b transcriptional factors and maintains the quiescence of QC cells (Kumpf et al., 2014). WUSCHEL-RELATED HOMEOBOX 5 (WOX5), a well-studied marker of QC, arises confinedly in the hypophysis of early globular embryo, slightly earlier than the period of QC birth. The WOX5 protein always keeps company with the QC development process from the embryonic stage to the postembryonic stage (Haecker et al., 2004). It is a well-known fact that the loss of WOX5 function causes partial loss of QC identity, premature differentiation of distal stem cells, and accelerated proliferative activity of QC cells (Burkart et al., 2019; Celine et al., 2014; Sarkar et al., 2007). Therefore, WOX5 not only plays a significant role in maintaining the quiescence of QC cells, but also acts as a central transcriptional factor of the SCN. However, how the QC permanently maintains the homeostasis of very low proliferative activity from the embryonic stage to the postembryonic stage remains unknown. WOX5 is a stereotypical transcriptional repressor with EAR motif. It targets several key downstream genes involved in the regulation of QC cell activity. For instance, WOX5 directly targets D-type cyclins and CDF4, the former promoting division of QC cells, and the latter facilitating differentiation of distal stem cells (Berckmans et al., 2020; Celine et al., 2014; Pi et al., 2015). Additionally, WOX5 indirectly regulates the expression of YUCCA1 (YUC1), SHR, CYCD6;1, which may be involved in regulating the mitotic activity of QC and initial cells (Clark et al., 2020; Savina et al., 2020; Tian et al., 2014). Several protein-protein interaction factors of WOX5, TOPLESS/TOPLESS-RELATED (TPL/TPR), HISTONE DEACETYLASE 19 (HDA19) and HAIRY MERISTEM (HAM), PLT, and BRASSINOSTEROIDS AT VASCULAR AND ORGANIZING CENTER (BRAVO) play important roles in the fate decision of distal stem cells and quiescence establishing of the QC (Burkart et al., 2019; Pi et al., 2015; Vilarrasablasi et al., 2014; Zhou et al., 2018). The direct upstream regulators of WOX5, REPRESSOR OF WUSCHEL1 (ROW1) grants the identity of QC by confining WOX5's expression to the QC cells, SEUSS (SEU) and SCR specify the QC by recruiting ASHR3 H3K36 methyltransferase SET DOMAIN GROUP 4 (SDG4) to activate WOX5's expression (Zhai et al., 2020; Zhang et al., 2015). The peptide CLAVATA3/ESR-RELATED 40 (CLE40) and its receptor ARABIDOPSIS CRINKLY4 (ACR4), coreceptors CLAVATA1 (CLV1) and CLV3 INSENSITIVE KINASES (CIKs) mediate the non-direct upstream signals of WOX5, then regulate the activity of QC cells and distal stem cells (Berckmans et al., 2020; Stahl et al., 2013; Stahl et al., 2009; Zhu et al., 2021). However, the

regulation of WOX5 protein homeostasis through post-translational modifications and its potential impact on the permanent maintenance of the low proliferative activity in quiescent center (QC) cells are still not understood.

Here, we identified a PEST domain in the WOX5 protein, which function remains undiscovered before in the WOX5 protein. Our investigation revealed that this PEST domain plays a crucial role in stabilizing the WOX5 protein, which in turn maintains the low proliferative activity of QC cells. Furthermore, we characterized that the PEST domain functions through the serine and/or threonine sites of GSK3 Motifs (GMs) in the PEST domain. Biochemical evidence demonstrated that the subfamily II of AtSKs (the homologs of GSK3) interact with WOX5 by phosphorylating the GMs. Genetic and chemical inhibition experiments demonstrated that the subfamily II AtSKs inhibit the proliferative activity of QC cells from the embryonic stage to the post-embryonic stage by stabilizing WOX5 protein. We further discovered that the subfamily II of catalytic subunit of *Arabidopsis* Protein Phosphatase 2A (AtPP2A-Cs) interact with WOX5. In the subfamily II of AtPP2A-Cs (*c3c4*) loss of function mutant, WOX5 protein has a significant increase in QC cells, stele initials (SI), and its daughter cells (SID), which causes the appearance of more QC-like cells. Contrarily, overexpressed the subfamily II of AtPP2A-Cs protein causes an increase of the proliferative activity of QC by dephosphorylating the phosphorylated WOX5 protein. Furthermore, we observed that treatment with a chemical inhibitor targeted against the subfamily II of AtSKs significantly reduces the elevated levels of WOX5 protein in the *c3c4* mutant. This finding strongly suggests that the increased WOX5 protein in *c3c4* is predominantly a phosphorylated form, specifically phosphorylated by the subfamily II of AtSKs. In addition, the proliferative activity of SI and SID also decreases in *c3c4*, but this decrease disappear in *c3c4wox5-1* triple mutant. Treatment with a specific chemical inhibitor targeted against the subfamily II of AtSKs results in an opposing effect, causing an increase in the proliferative activity of QC cells, as well as SI and SID cells in *c3c4*. These results reveal that increasing phosphorylated WOX5 protein is required for reducing the proliferative activity of QC, SI, and SID in *c3c4*. Moreover, in situ overexpressed WOX5 protein in QC cells, SI and SID recapitulated the phenotypes in *c3c4*. Most importantly, the dynamic induction assay directly testify that accumulated WOX5 protein in QC can reduce its proliferative activity, and accumulated WOX5 protein in SI and SID cells can reduce their proliferative activity and convert these cells into QC-like cells at the postembryonic stage. These data prove that increased WOX5 protein in QC cells and SI and SID is sufficient for reducing their proliferative activity. The phosphate-mimicked WOX5 protein partially reproduces the phenotypic characteristics observed in *c3c4*. However, treatment with a chemical inhibitor specifically targeting the subfamily II of

AtSKs does not lead to destabilization of the mimicked phosphorylated WOX5 protein, nor does it induce an increase in the proliferative activity. These results testify that phosphate-mimicked WOX5 protein is also sufficient for reducing the proliferative activity.

In summary, our study uncovers that phosphorylation of WOX5 protein by the subfamily II of AtSKs controls the low proliferative activity of QC. Oppositely, the subfamily II AtPP2A-Cs enhances the proliferative activity of QC cells by dephosphorylating WOX5 protein. Additionally, the subfamily II AtPP2A-Cs maintains just one-layer QC cells by downregulating the WOX5 expression and destabilizing WOX5 protein in SI and SID. Taken together, reversible phosphorylation of WOX5 protein not only controls the homeostasis of the low proliferative activity in QC cells, but also controls the homeostasis of one-layer QC from the embryonic stage to the postembryonic stage in *Arabidopsis*.

Results:

The PEST domain stabilizes WOX5 protein and maintains low proliferative activity of QC cells

Previous methods for identifying and imaging the QC, such as X-irradiation, β-rediation, autoradiography, nucleoside analogs BrDU immunodetection, and EdU click reaction, have some shortcomings (Clowes, 1961, 1963; Dolan et al., 1993; Kotogány et al., 2010). These methods can't present the most natural proliferative activity because they may stimulate proliferation of QC cells. Additionally, they are static. The 4D imaging method indicates that QC cells maintain low proliferative activity (cell division intervals almost 110 hours) in Columbia-0 (Col-0) ecotype (Rahni and Birnbaum, 2019). However, this dynamic method is not convenient to use in combining with other genetic materials. The 3D quantitative analysis can visualize the number, volume, and division pattern of QC cells, but this method is complicated (Lu et al., 2021). In order to describe the phenotype of the proliferative activity of QC more easily and more directly, we firstly introduce the index Proliferative Activity (PA) for defining the proliferative activity of QC. PA is the number of dividing QC cells per root at the stage of mature embryo or 5 days after germination (DAG). Cell plate on the longitudinal section is a natural marker showing the dividing cells. For getting the real PA of QC as much as possible, we count the cell plates of dividing QC cells (marked as D_{cp} equals the sum of the number of dividing QC cells of all the root tips) by viewing a mass of mature embryos (marked as N_e equals the number of all the mature embryos) and root tips (marked as N_r equals the number of all the root tips). So the PA equals D divided by N (the formulas are $PA_r = D_{cp} / N_r$ and $PA_e = D_{cp} / N_e$).

It is very difficult to investigate the regulation of WOX5 protein level since the very low WOX5 protein content exists in the root tips of *Arabidopsis*. Thus, we analyzed the protein sequence of WOX5 and its homolog WUSCHEL (WUS) in silico through the ePESTfind prediction website of http://embossgui.sourceforge.net/demo/manual/epestfind.html (Figure S1) (Rechsteiner and Rogers, 1996; Rogers et al., 1986). The output revealed a potential PEST domain with 18 amino acids between position 152 and 171 of WOX5 protein sequence, which PEST score was +6.02 (greater than threshold value +5.00 means a possible PEST domain with real interest). But the output showed no potential PEST domain in the WUS protein sequence (Figure S1), the results are consistent with previous report (Dolzblasz et al., 2016). However, the function of PEST domain remains unidentified. Meanwhile, the low hydrophobicity index of 40.36 (Figure S1) indicated that the PEST domain might be surface exposed and be accessible for the serine and/or threonine phosphorylation or protein-protein interaction (Meyer et al., 2011). Since C-terminal green fluorescent protein (GFP) fused WOX5 protein and N-terminal GFP fused WUS protein are the functional protein (Pi et al., 2015; Rodriguez et al., 2016; Yadav et al., 2011). To explore the possible function of the PEST domain for regulating the WOX5 protein, we thus introduced the WOX5-GFP, WOX5△PEST-GFP (full length WOX5 protein deletes PEST domain) and GFP-WUS fusion protein into *wox5-1* driving by the full-length promotor of WOX5 (Figure S2) for obtaining 10-15 rescued T_1 lines separately. We randomly selected 4 homozygous lines (named as W5-1~W5-4, dP-1~dP-4, WU-1~WU-4 separately) (Figure S3A) to perform semi-quantitative reverse transcription PCR (sqRT-PCR) and quantitative real time PCR (qPCR) assays. We identified 6 rescued lines (W5-3, W5-4, dP-2, dP-3, WU-1, WU-2 separately) with almost equal level of GFP expression (Figure S3), then we counted the PA_e at the mature embryonic stage and the PA_r at 5 DAG of the 6 rescued lines and *wox5-1*. The PA_e (=0.028) and PA_r (=0.129) of WOX5-GFP/*wox5-1* rescued lines was significantly lower than the PA_e (=0.640) and PA_r (=0.694) of WOX5△PEST-GFP/*wox5-1* lines (Figure 1A,B,F,G,H,I), the PA_e (=0.640) and PA_r (=0.694) of WOX5△PEST-GFP/*wox5-1* rescued lines markedly lower than the PA_e (=1.234) and PA_r (=1.917) of GFP-WUS/*wox5-1* rescued lines (Figure 1B,C,F,G,I,J), the PA_e (=1.234) and PA_r (=1.917) of GFP-WUS/*wox5-1* lines extremely lower than the PA_e (=1.976) and PA_r (=3.023) of *wox5-1* (Figure 1C,D,F,G,J,K). The results indicated that WOX5-GFP protein with the PEST domain could rescue the PA_e and PA_r of *wox5-1* up to almost equal to the wild type (WT) (Col-0 ecotype) (Figure 3A,H), however, WOX5△PEST-GFP protein and GFP-WUS protein, both are without the PEST domain, could not completely rescue the PAe and PAr of *wox5-1*. At the same time, we

quantified the fluorescence of GFP fusion protein in the QC zone at 5 DAG of the 6 lines and *wox5-1* (the value of blank background) (Figure 1D,E). The intensity of WOX5-GFP fusion protein was markedly higher than the intensity of WOX5△PEST-GFP and GFP-WUS fusion protein (Figure 1A~C,E), revealed that the PEST domain stabilizes WOX5 protein. Further analysis revealed that tandem three GMs (S/T-X-X-X-S/T^{-P}) (named GM3, GM4 and GM5) (Fiol et al., 1990; Youn and Kim, 2015) exists in the PEST domain, in addition, other two GMs (named GM1 and GM2) in the protein sequence of WOX5 out of the PEST domain (Figure S4). Previous studies had shown that the S/T sites at the N terminal of the GMs were the real phosphorylation sites being phosphorylated by GSK3s, but the S/T sites at the C terminal of the GMs are the primed phosphorylation sites being phosphorylated by other kinases (Ali et al., 2001; Patel and Woodgett, 2017). Thus, to investigate which GMs are involved in regulating stability of WOX5 protein and the QC's proliferative activity. We constructed five plasmids (WOX5mGM1-GFP, WOX5mGM2-GFP, WOX5mAll-GFP, WOX5m5A-GFP, and WOX5m3A-GFP) using site-directed mutagenesis, these plasmids were also introduced into *wox5-1*. We then randomly selected 4 homozygous lines (named mGM1-1~mGM1-4, mGM2-1~mGM2-4, mAll-1~mAll-4, m5A-1~m5A-4, and m3A-1~m3A-4 separately) (Figure S5) from descendants of 10-15 rescued T_1 lines to perform sqRT-PCR and qPCR assays, we identified 10 rescued lines (mGM1-1, mGM1-4; mGM2-1, mGM2-2; mAll-2, mAll-3; m5A-1, m5A-2; m3A-2, m3A-3 separately) with almost equal GFP expression (Figure S5). We next also counted the PA_e at the mature embryonic stage and the PA_r at 5 DAG of the 10 rescued lines. The PA_e and PA_r of WOX5mGM1-GFP/*wox5-1* rescued lines and WOX5mGM2-GFP/*wox5-1* rescued lines were similar to WOX5-GFP/*wox5-1* rescued lines (Figure S6A,B,G,H,I,J). The PAe/ PAr of WOX5mAll-GFP/wox5-1 , WOX5m5A-GFP/wox5-1 , and WOX5m3A-GFP/wox5-1 rescued lines were significantly higher than the WOX5mGM1-GFP/wox5-1 and WOX5mGM2-GFP/wox5-1 rescued lines (Figure S6A~C,G~M), indicating that GM3,GM4 and GM5 in the PEST domain rather than GM1 and GM2 inother domains of wox5 play a crucial role in maintaining the low proliferative activity of QC.. Meanwhile, we quantified the fluorescence of GFP fusion protein in the QC zone at 5 DAG of the 10 rescued lines. The intensity of WOX5mGM1-GFP and WOX5mGM2-GFP fusion protein were significantly higher than the intensity of WOX5mAll-GFP, WOX5m5A-GFP, and WOX5m3A-GFP fusion protein (Figure S6A~F), which revealed that GM3, GM4 and GM5 , instead of GM1 and GM2, are critical for stabilizing WOX5. Taken together, the GMs in the PEST domain stabilizes WOX5 protein and maintains the low proliferative activity of QC cells.

In addition, we introduced the WOX5-GFP, WOX5△PEST-GFP, GFP-WUS, WOX5mGM1-GFP, WOX5mGM2-GFP, WOX5mAll-GFP, WOX5m5A-GFP, and WOX5m3A-GFP fused protein into QC184/*wox5-1* line for obtaining homozygous lines. The β-glucuronidase (GUS) staining for 48-72 hours showed WOX5-GFP/QC184/*wox5-1* (40/42), WOX5mGM1-GFP/QC184/*wox5-1* (40/43), and WOX5mGM2-GFP/ QC184/*wox5-1* (36/38) lines completely rescued the GUS activity of QC184/*wox5-1* (36/36) line almost be equal to QC184 (27/28) (Figure S7A~E). However, GFP-WUS/ QC184/ *wox5-1* (31/54), WOX5△PEST-GFP/ QC184 /*wox5-1* (29/54), WOX5mAll-GFP/ QC184/ *wox5-1* (31/55), WOX5m5A-GFP/ QC184/ *wox5-1* (25/42), and WOX5m3A-GFP/ QC184/ *wox5-1* lines (28/47) partially rescued the GUS activity of QC184/*wox5-1* (Figure S7F~O). These results indicate that increased QC proliferative activity causes a decrease of QC184 GUS activity.

The subfamily II of AtSKs interact with WOX5 in the QC cells

In mammals, glycogen synthase kinase-3 (GSK3s) are involved in almost all pathways including Insulin signalling pathway (glycogen metabolism), Notch signalling pathway (tissue patterning and cell polarity), Transforming Growth Factor β (TGFβ) signalling pathway (proliferation and differentiation), and canonical Wnt/β-catenin pathway (stem cell pluripotency and self-renewal) (Patel and Woodgett, 2017). In plants, GSK3s also are involved in many important pathways, such as brassinosteroid (BR) signalling pathway, ABA signalling pathway, Auxin signalling pathway, stomatal development and stress response (Houbaert et al., 2018; Li et al., 2020; Youn and Kim, 2015). However, whether GSK3s regulate root stem cell pluripotency and self-renewal needs to be clarified. There are 10 GSK3s in *Arabidopsis* (AtSKs), also known as SHAGGY-like kinases (Youn and Kim, 2015), since only mutated the GMs in the PEST domain of WOX5 could be almost equal to the role of truncation of PEST domain in regulating the QC proliferative activity and the stability of WOX5 protein (Figure 1 and Figure S6). Hence, we want to figure out which GSK3s may be involved in phosphorylating WOX5 protein. Firstly, we performed sqRT-PCR assay, the results showed that all ten AtSKs express in the one centimeter root tips of Col-0 at 5 DAG (Figure S8). Next, we obtained all transcriptional reporters of ten AtSKs (Figure S8) We found that only the subfamily I(AtSK11, AtSK12,AtSK13), subfamily II (AtSK21, AtSK22, AtSK23) of AtSKs, and AtSK32 expressed in the QC (Figure S9 and Figure 2A). Meanwhile, we used the yeast 2-hybrid (Y2H) assay to screen all AtSK proteins for interactions with the WOX5 protein. The results revealed that only the subfamily II of AtSKs (ATSK21, ATSK22 and ATSK23) have the weak interaction with WOX5 (Figure 2B). On the whole, only the subfamily II of AtSKs may interact with WOX5 in root tips. To further testify that the subfamily II of

AtSKs interact with WOX5, we performed bimolecular fluorescent complimentary (BiFC) in the *nicotiana tabacum*. The results showed that the positive control HAIRY MERISTEM 4(HAM4) interacts with WOX5 (Figure S10A) (Zhou et al., 2018), the members of subfamily II of AtSKs (ATSK21, ATSK22, and ATSK23) interact with WOX5 (Figure 2C), the negative control RGA not interacts with WOX5 (Figure S10B), and AtSK21 not interacts with WUS (Figure S10C). Owing to the three proteins of the subfamily II of AtSKs share very high amino acid sequence similarity (Figure S11), so we selected AtSK21 as a representative for the following assays. Pull-down in vitro assays revealed MBP-WOX5 interacts with GST-AtSK21, but MBP-WOX5 not interacts with GST, and MBP not interacts with GST and GST-AtSK21 (Figure 2D). Finally, we combined p35S:Flag-AtSK21/Col-0 (He et al., 2019) with p35S:LhGR-pOp:WOX5-YFP/Col-0 (Pi et al., 2015) for obtaining the double homozygous line, thereafter we performed co-immunoprecipitation (CoIP) in vivo using GFP beads for enriching WOX5-YFP fusion protein, the input proteins and immunoprecipitation protein detected by immunoblotting using anti-Flag and anti-GFP antibodies. The data revealed that AtSK21 protein can interact with WOX5 protein in *Arabidopsis* (Figure 2E). Taken together, the subfamily II of AtSKs interacts with WOX5 in vitro and in vivo.

WOX5 is epistatic to the subfamily II of AtSKs in inhibiting the proliferative activity of QC cells

To figure out whether the subfamily II of AtSKs are involved in regulating proliferative activity of QC cells, and to testify the genetic connection between WOX5 and the subfamily II of AtSKs, we combined the *wox5-1* and *atsk21/22/23* (Yan et al., 2009) for obtaining the quadruple mutant (*atsk21/22/23/wox5-1*). Thereafter, we counted the PAe and PAr of a lot of mature embryos and root tips of WT, *wox5-1*, *atsk21/22/23* and *atsk21/22/23/wox5-1* by using the improved mPS-PI staining technique (Truernit et al., 2008). The PAr and PAe of Col-0 are very low as 0.071 and 0.059, which is remarkably lower than the value of *wox5-1* that equal to 2.803 and 2.203. (Figure 3A,B,F,G,H,I). This result revealed that WOX5 maintains the low proliferative activity of QC cells, which is consistent with previous reports (Burkart et al., 2019; Celine et al., 2014). The PAr and PAe of *Wassilewskija* (Ws) (the WT of *atsk21/22/23*) are low as 0.273 and 0.073, which is remarkably lower than the PAr and PAe of *atsk21/22/23* (equal to 1.396 and 0.731) (Figure 3C,D,F,G,J,K). This result revealed that the subfamily of AtSKs also inhibit the proliferative activity of QC cells. The PAr and PAe of *wox5-1/atsk21/22/23* are very high as 2.831 and 2.053, which is not different with the PAr and PAe of *wox5-1* (Figure 3E,F,G,L). This result indicates that WOX5 is epistatic to the subfamily II of AtSKs in inhibiting the proliferative activity of QC cells. A small molecule, Bikinin (Bik), acts as an ATP competitor, which inhibits kinase activity

of seven AtSKs (AtSK11, AtSK12, AtSK13, AtSK21, AtSK22, AtSK23, AtSK31) (De Rybel et al., 2009). To determine the optimum concentration of Bik for inhibiting the kinase activity of the subfamily II of AtSKs, we planted Col-0 and Ws on the ½ MS medium (containing 1% agar and 1% sucrose) with 0 (DMSO, the Mock), 15 and 30 μM Bik. We found that treating with the 30 μM Bik (Figure S12A,B,D,G), rather than the Mock and the 15 μM Bik treatment (Figure S12C,E,F), could simulate the downward spiral root tips phenotypes of *atsk21/22/23* root tips that like the instant noodles. Thus, we simultaneously planted Col-0, Ws and *wox5-1* on the ½ MS medium containing 30 μM Bik or with DMSO (the Mock). Compared to the Mock, treating with the 30 μM Bik, the value of PAr of Col-0 significantly increased from 0.245 to 1.712 ,while Ws increased from 0.245 to 1.547 (Figure S13A~D,G), which had almost no difference with the PAr of *atsk21/22/23* (Figure S13H). These results also that 30 μM Bik treatment can mimic the increased QC proliferative activity of *atsk21/22/23*, and it was only the subfamily II of ten AtSKs that involved in inhibiting proliferative activity of QC cells. However, treating with the 30uM Bik, the PAr of *wox5-1* almost had no difference with the Mock (from 2.771 to 2.875) (Figure S13E~G), which also indicated that WOX5 is epistatic to the subfamily II of AtSKs in maintaining low proliferative activity of QC cells.

In addition, we planted the QC184 line, QC184/*wox5-1* line and QC25 line, QC25/*wox5-1* line on the ½ MS medium with 30 μM Bik or Mock. We took GUS staining using 5DAG root tips, the GUS activity in the QC of QC184 line and QC25 line on the Mock are higher than on the 30 μM Bik (Figure S14A,C,E,G), however, in the *wox5-1* backgroud, the QC cells' GUS activity of QC184 and QC25 with 30 μM Bik treatment is not different from the Mock (Figure S14B,D,F,H). The results indicated that increased QC proliferative activity causes a decrease of QC184/QC25 GUS activity and WOX5 is epistatic to the subfamily II of AtSKs in maintaining the identity of QC.

The subfamily II of AtSKs inhibit the proliferative activity of QC cells by phosphorylating and stabilizing the WOX5 protein

Since the subfamily II of AtSKs and WOX5 protein interact in inhibiting the proliferative activity of QC cells, we want to figure out how these kinases regulate the WOX5 protein in the QC cells. Therefore, we performed the sqRT-PCR and qPCR assays, in contrast to the Ws, the mRNA level of WOX5 got no change in the *atsk21/22/23* (Figure S15A,B), suggesting that the subfamily II of AtSKs does not affect the transcriptional level of WOX5 in *Arabidopsis*. We then combined stable homozygous lines of pWOX5:nlsGFP/Col-0 and pWOX5:WOX5GFP/Col-0 (Pi et al., 2015) to Ws and *atsk21/22/23*, quantification of GFP fluorescence in the QC at the 5DAG root tips showed that the expression level of WOX5 in *atsk21/22/23* was not different to in Ws (Figure

4A,B,C), however, the protein level of WOX5 in *atsk21/22/23* was markedly lower than in Ws (Figure 4D,E,F). Moreover, we treated the pWOX5:nlsGFP/Col-0 and pWOX5:WOX5GFP/Col-0 lines with 30 μM Bik (the DMSO as the Mock) for 5 days. The quantification of GFP fluorescence in the QC also revealed that the WOX5's expression level of pWOX5:nlsGFP/Col-0 on the Mock was not different to on 30 μM Bik (Figure S16A,B,E), but the WOX5's protein level of pWOX5:WOX5GFP/Col-0 on the Mock was markedly higher than on 30 μM Bik (Figure S16C,D,F). These data indicate that the subfamily II of AtSKs stabilizes WOX5 protein in the QC cells, and the reducing WOX5 protein causes the increase of the proliferative activity of QC cells (Figure S13E,F,G) and the decrease of QC184/QC25 GUS activity (Figure S14A,C,E,G).

According to the Figure S6 and the Figure 4A~F, we concluded that the GMs in the PEST domain stabilizes WOX5 protein and the subfamily II of AtSKs stabilizes WOX5 protein. Thus, we speculate that the subfamily II of AtSKs stabilizes WOX5 protein by phosphorylating the GMs in the PEST domain. To testify this speculation, on one hand, we constructed three plasmids (WOX5-GFP, WOX5m5D-GFP, WOX5m3D-GFP) (Figure S17A) by using site-directed mutagenesis, they were introduced into *atsk21/22/23*, we selected 4 homozygous lines (named W5-1~W5-4, 5D-1~5D-4, 3D-1~3D-4 separately) randomly from descendants of 10-15 T_1 phosphate-mimicked lines to perform sqRT-PCR and qPCR assays, we identified 6 lines (W5-1, W5-2; 5D-1, 5D-2; 3D-1, 3D-2 separately) with almost equal GFP expression (Figure S17B,C,D). We next counted the PA_e at the mature embryonic stage and the PA_r at 5 DAG of these 6 phosphate-mimicked lines. The PA_e and PA_r of the WOX5m3D-GFP/*atsk21/22/23* lines and WOX5m5D-GFP/*atsk21/22/23* lines were similar to the Ws (Figure S18) and were significantly lower than the WOX5-GFP/*atsk21/22/23* lines (Figure 4G~J, L~O), which indicated that these phosphate-mimicked lines could rescue the phenotype of *atsk21/22/23*. Meanwhile, we quantified the fluorescence of GFP fusion protein in the QC zone at 5 DAG of the 6 lines. The intensity of WOX5m5D-GFP and WOX5m3D-GFP fusion protein were markedly higher than WOX5-GFP fusion protein (Figure 4G~I, K), which revealed that these phosphate-mimicked WOX5 protein could rescue the stability of WOX5 protein in the *atsk21/22/23*, suggesting that the subfamily II of AtSKs stabilizes WOX5 protein by phosphorylating the GMs in the PEST domain, and indicating that increased WOX5 protein can reduce the PA of QC. On the other hand, we constructed prokaryotic expression vectors of GST-AtSK21, GST-AtSK21(K69R) (the kinase dead type), MBP-WOX5, MBP-WOX5△PEST, MBP-WOX5mAll, MBP-WOX5m5A, MBP-WOX5m3A and MBP-BZR1 (the positive control) (He et al., 2002), we purified these tagged protein using MBP beads and GST beads, the images of CBB staining showed that we obtained

the purified MBP-BZR1, MBP, MBPWOX5, MBPWOX5△PEST, MBP-WOX5mAll, MBP-WOX5m5A, MBP-WOX5m3A substrate proteins and GST-AtSK21, GST-AtSK21(K69R) kinase proteins (Figure S19A). Thereafter, we performed kinase assay in vitro, and then running proteins in the Mn^{2+} Phos-tag SDS-PAGE after terminating kinase reaction, the experiment group showed that GST-AtSK21 could phosphorylate MBP-WOX5 (Figure S19C), but could not phosphorylate MBP-WOX5△PEST, MBP-WOX5mAll, MBP-WOX5m5A, MBP-WOX5m3A (Figure S19C), GST-AtSK21(K69R) also could not phosphorylate MBP-WOX5 (Figure S19C). In conclusion, the subfamily II of AtSKs stabilizes WOX5 protein by phosphorylating the GMs in the PEST domain. Taken together, (the subfamily II of AtSKs-) phosphorylated WOX5 protein inhibits proliferative activity of QC cells and maintains identity of QC.

The subfamily II of AtPP2A-Cs interact with WOX5 in the QC cells

Since AtSKs stabilize WOX5 protein by phosphorylating the GMs, we speculate that phosphatases may antagonize phosphorylation of AtSKs by dephosphorylating the GMs, therefore maintain the homeostasis of WOX5 protein in the QC. In mammals, the Wnt/β-catenin signalling pathway plays a crucial role in regulating pluripotency and proliferative activity of stem cell (Clevers et al., 2014; Sokol, 2011). β-catenin serves as a central component of the Wnt/β-catenin signalling pathway, which homeostasis is phosphorylated by GSK3 and dephosphorylated by PP2A holoenzyme, regulates the activity of downstream central transcriptional factors (TFs) (MacDonald et al., 2009; Su et al., 2008). In *Arabidopsis*, the QC is required for maintaining the homeostasis of SCN and is the source of stem cells. WOX5, which serves as the central TF for maintaining the activity of QC, whether its homeostasis is regulated by the pair of antagonists (GSK3s and PP2As) remains unknown. Thus, we focus on five members of AtPP2A-Cs family owing to the catalytic subunit of PP2A holoenzyme is required for dephosphorylation (Shi, 2009). We want to figure out which AtPP2A-Cs in the *Arabidopsis* may be involved in dephosphorylating WOX5 protein. Firstly, we performed sqRT-PCR assay, the results showed that all five AtPP2A-Cs expressed in the one centimeter root tips of Col-0 at 5 DAG (Figure S20). Next, we obtained all transcriptional reporters of five AtPP2A-Cs in Col-0 ecotype including subfamily I (pC1:nlsGFP, pC2:nlsGFP, pC5:nlsGFP); subfamily II (pC3:nls3×GFP, pC4: nls3×GFP). We found that only AtPP2A-C3, AtPP2A-C4, AtPP2A-C5 expressed in the QC (Figure 5A). Meanwhile, we constructed WOX5 on the BD and five AtPP2A-Cs on the AD for Y2H assays, the results revealed that AtPP2A-C1, AtPP2A-C2, AtPP2A-C3 and AtPP2A-C4 have strong interaction with WOX5 just like the positive control of WOX5 and TPR1 (Figure 5B) (Pi et al., 2015), and the AtPP2A-C5 have no interaction with

WOX5, and the negative control RGA have no interaction with WOX5 (Figure 5B). On the whole, only the subfamily II of AtPP2A-Cs (AtPP2A-C3 and AtPP2A-C4) may interact with WOX5 in root tips. To further testify that subfamily II of AtPP2A-Cs (AtPP2A-C3 and AtPP2A-C4) interact with WOX5, we performed BiFC in the *nicotiana tabacum*, the results indicated that the positive control HAM4 interacts with WOX5 (Zhou et al., 2018) (Figure S10A), the subfamily II of AtPP2A-Cs (AtPP2A-C3 and AtPP2A-C4) interacts with WOX5 (Figure 5C), the negative control RGA not interacts with WOX5 (Figure S10B) and AtPP2A-C3 not interacts with WUS (Figure S10D). Thereafter, MBP pull-down in vitro assays revealed MBP-WOX5 interacts with GST-C3 and GST-C4 (Figure 5D). Finally, we generated the transgenetic homozygous lines of 35S : Flag-C3/Col-0 and 35S : Flag-C4/Col-0, then we combined them with 35S : LhGR-pOp : WOX5-YFP/Col-0 (Pi et al., 2015) line for obtaining the double homozygous lines of 35S : Flag-C3/Col-0×35S : LhGR-pOp : WOX5-YFP/Col-0 and 35S : Flag-C4/Col-0×35S : LhGR-pOp : WOX5-YFP/Col-0 separately. Thereafter we performed CoIP in vivo. The results revealed that AtPP2A-C3 and AtPP2A-C4 proteins can interact with WOX5 protein in *Arabidopsis* (Figure 5E). Taken together, the subfamily II of AtPP2A-Cs interacts with WOX5 in vitro and in vivo.

The subfamily II of AtPP2A-Cs increased the proliferative activity of QC cells by dephosphorylating and destabilizing the WOX5 protein

Given that the subfamily II of AtSKs inhibit the proliferative activity of QC cells by phosphorylating and stabilizing the WOX5 protein (Figure 4, Figure S19), and the subfamily II of AtPP2A-Cs interacts with WOX5 protein (Figure 5). So we want to figure out whether the subfamily II of AtPP2A-Cs can increase the proliferative activity of QC cells by dephosphorylating and destabilizing the WOX5 protein. Therefore, performed sqRT-PCR and qPCR using the cDNA from the mutant of loss function of the subfamily II of AtPP2A-Cs (*c3c4*) (Spinner et al., 2013) or Col-0. In contrast to the Col-0, the WOX5 expression level increased almost 1.5 times in the *c3c4* (Figure S21A). We then combined pWOX5:nlsGFP/Col-0 and pWOX5:WOX5GFP/Col-0 (Pi et al., 2015) with *c3c4*. Quantification of GFP fluorescence in the QC at the 5DAG root tips demonstrated that the expression level of WOX5 in the QC of *c3c4* was comparable to that in Col-0 (Figure 6A~D,I). However, quantification of GFP fluorescence in the SI and SID at the 5DAG root tips showed that the expression level of WOX5 in the SI and SID of *c3c4* was markedly higher than Col-0 (Figure 6A~D,I). These data indicate that the increased abundance of WOX5 mRNA is derived from the SI and SID, rather than from the QC cells in *c3c4* mutants. We then quantified the protein levels of WOX5 in Col-0 and *c3c4* plants by measuring the GFP fluorescence in the QC, SI and SID at the 5DAG root tips. The results showed

that the GFP fluorescence in the QC and SI of *c3c4* was significantly higher than that in Col-0 (Figure 6E~H,J). These results suggest that loss of function of the subfamily II of AtPP2A-Cs increased the content of WOX5 protein in the QC by enhancing the stability of WOX5 protein, and increased the content of WOX5 protein in the SI and SID by increasing the mRNA content of WOX5 and/or by enhancing the stability of WOX5 protein. Thus, the subfamily II of AtPP2A-Cs destabilizes WOX5 protein.

WOX5 protein reduced in QC cells of *atsk21/22/23* (Figure 4D~F), but WOX5 protein increased in QC cells of *c3c4* (Figure 6E~H,J). Consequently, we speculate that the subfamily II of AtPP2A-Cs may promote the proliferative activity of QC cells by dephosphorylating the GMs being phosphorylated by the subfamily II of AtSKs. To testify this speculation, firstly, we generated the transgenetic homozygous lines of 35S : AtPP2A-C3-GFP/Col-0 and 35S : AtPP2A-C4-GFP/Col-0, we extracted the total proteins of 2 centimeters root tips of 35S : AtPP2A-C3-GFP/Col-0 line and 35S : AtPP2A-C4-GFP/Col-0 line at 5 DAG, we next used GFP beads to purify the holoenzymes of AtPP2A-C3-GFP and AtPP2A-C4-GFP. The result of immunoprecipitation of anti-GFP showed that we obtained the holoenzymes of AtPP2A-C3-GFP and AtPP2A-C4-GFP (Figure 6Q). Subsequently, we conducted in vitro dephosphorylation assays and utilized Phos-tag-Mn^{2+}-SDS-PAGE to separate phosphorylated proteins. Similarly to lambda protein phosphatases (Lambda PP), the holoenzymes of AtPP2A-C3-GFP and AtPP2A-C4-GFP were also able to dephosphorylate the (GST-AtSK21-) phosphorylated MBP-WOX5 protein (Figure 6W). In addition, we observed and quantified the PAr of 35S:AtPP2A-C3-GFP/Col-0 and 35S:AtPP2A-C4-GFP/Col-0 overexpressed lines, in comparison to Col-0, all of these lines exhibited significantly increased PAr (Figure 6K,M,N). Furthermore, we overexpressed AtPP2A-C3-GFP and AtPP2A-C4-GFP protein by using GAL4-VP16 transcriptional activator driving by the full-length promotor of WOX5 genomic sequence, followed 6 multiple upstream activation sequence (6×UAS) (pWOX5:GAL4-VP16-6×UAS: CDS-GFP, abbreviated as GVUAS:CDS-GFP here after) (Figure S22). Compared to Col-0, all the specific overexpressed lines also showed a significant increase in PAr (Figure 6L,O,P). These findings suggest that overexpression of subfamily II of AtPP2A-Cs proteins can enhance the proliferative activity of QC. In summary, the subfamily II of AtPP2A-Cs plays a role in reducing the WOX5 protein in QC, SI, and SID, thereby increasing the proliferative activity of QC cells through the dephosphorylation of (the subfamily II of AtSKs-) phosphorylated WOX5 protein.

WOX5 is necessary for producing more quiescent cells when loss of function the subfamily II of AtPP2A-Cs

Since loss of function of the subfamily II of AtPP2A-Cs increased WOX5 protein in QC, SI, and SID (Figure 6F~H,J), we reason that the phenotypes of *c3c4* mutant might appear more quiescent cells. To testify this reasoning, firstly, we noticed that the 5 DAG seedling of *c3c4* in the ½ MS medium present several different phenotypes including short root (22.60%), shorter root (37.57%), shortest root (33.05%) and three cotyledons (6.78%) (Figure S23). Thus, we viewed the root tips and mature embryos of *c3c4* carefully, the root tips at 5 DAG also have several phenotypes including (here we firstly named as) two layers QC-like cells (41.11%) (Figure 7B), more and wider QC-like cells (33.33%) (Figure 7C), one layer QC cells (25.56%) (Figure 7D), the mature embryos also have several phenotypes including two layers QC-like cells (36.36%) (Figure 7H), more and wider QC-like cells (35.06%) (Figure 7I), one layer QC (28.57%) (Figure 7J). Compared to Col-0 (Figure 7A,G), the significantly increased abnormal phenotypes in two layers of QC-like cells and the presence of more and wider QC-like cells suggest that in the *c3c4* , the proliferative activity of QC cells doesn't change, but instead produces more QC-like cells originating from SI and SID. Then, we view the root tips of *c3c4* by using another method of EdU (5-ethynyl-2'-deoxyuridine)-based S-phase assay (Kotogány et al., 2010) because the cell plates of SI and SID are not convenient to counting. We transplanted the 4DAG seedling of *c3c4* to ½ MS with 2.5 μM EdU for 12 hours. After EdU staining, compare with the images of one layer nondividing cells without EdU incorporation signal (95.59%) of WT (Figure 7M), the images of *c3c4* mutant can also be classified into three types including (here we firstly named as) two layers nondividing cells without EdU incorporation signal (33.58%) (Figure 7N), more and wider nondividing cells (38.06%) without EdU incorporation signal (Figure 7O), and one layer nondividing cells (28.36%) without EdU incorporation signal (Figure 7P). These results showed that the QC proliferative activity of the *c3c4* is similar to that of the WT, but the proliferative activity of SI and SID of *c3c4* is significantly lower than that of the WT. These data demonstrate that increased WOX5 protein in QC (Figure 6F~H,J) still maintains quiescence of QC cells, but increased WOX5 protein in SI and SID (Figure 6F~H,J) reduces the PA of SI and SID, therefore produced more quiescent cells.

Since the reduced WOX5 protein in atsk21/22/23 cause a decline of GUS activity QC184 and QC25 (Figure 4D~F, Figure S14A,C,E,G), we speculate that increased WOX5 protein in *c3c4* can lead to an increase in GUS activity of QC184 and QC25. Thus, we combined QC25 and QC184 with *c3c4* for obtaining QC25/*c3c4* and QC184/*c3c4* homozygous lines. After GUS staining assay, compare with just one layer blue cells of QC184 (100%) (Figure 7S), the

phenotypes of QC184/*c3c4* can be divided into three types including (here we firstly named as) two layers blue cells (37.04%) (Figure 7T), more and wider blue cells (30.25%) (Figure 7U) and one layer blue cells (31.48%) (Figure 7V), and the GUS activity in QC of almost all QC184/*c3c4* is markedly higher than QC184. Likewise, compare with just one layer blue cells of QC25 (95.56%) (Figure S24A), the phenotypes of QC25/*c3c4* can also be divided into three types as above, including two layers blue cells (33.77%) (Figure S24B), more and wider blue cells (34.42%) (Figure S24C) and one layer blue cells (31.82%) (Figure S24D), and the GUS activity in QC of almost all QC25/*c3c4* is markedly higher than QC25. The results suggest that increased WOX5 protein in QC of *c3c4* (Figure 6F~H,J) can increase GUS activity of QC184 and QC25, and increased WOX5 protein in SI and SID (Figure 6F~H,J) of *c3c4* can also enhance GUS activity of QC184 and QC25.

To further testify that WOX5 is necessary for producing more quiesent cells and increasing GUS activity of QC184 and QC25. We further combined *wox5-1* with *c3c4* and QC25/*c3c4* and QC184/*c3c4* for obtaining homozygous lines of *c3c4wox5-1*, QC25/*c3c4wox5-1*, QC184/*c3c4wox5-1*. After mPS-PI viewing and EdU staining, the results show that the phenotypes of high PA cells and one layer dividing cells of almost all *c3c4wox5-1* (Figure 7F,L) do not exhibit any significant deviations from that of the *wox5-1* (Figure 7E,K) from the embryonic stage to the post-embryonic stage. After GUS staining, the lack of GUS activity (here we named as one layer not blue cells) of QC184/*c3c4wox5-1* (Figure 7X) is not different from that in QC184/*wox5-1* (Figure 7W), and the low QC GUS activity (here we named as one layer light blue cells) of QC25/*c3c4wox5-1* (Figure S24E) is not different from that in QC25/*wox5-1* (Figure S24F). These data suggest that WOX5 is necessary for producing more quiescent cells and for increasing GUS activity of QC184 and QC25 in *c3c4* background.

To demonstrate the requirement of phosphorylated WOX5 protein in producing additional quiescent cells and elevating GUS activity of QC184 and QC25 in the absence of subfamily II of AtPP2A-Cs. We used 30 μM Bik to processing genetic materials of pWOX5:nlsGFP/*c3c4* and pWOX5:WOX5GFP/*c3c4*. Compared to the Mock, the GFP intensity in QC, SI, and SID regions of transcriptional reporter exposed to the 30 μM Bik are not changed (Figure S25A~F,N). However, the GFP intensity in the same regions of the protein reporter markedly decreased (Figure S25G~M,O), indicating that increased WOX5 protein in *c3c4* mainly is the phosphorylated WOX5 protein. Additionally, these phosphorylated WOX5 protein gradually degraded when the kinase activity of subfamily II of AtSKs is continuously inhibited using 30 μM Bik. Therefore, we next used 30 μM Bik to processing genetic material of *c3c4* mutant and viewed the root tips by using the mPS-PI method, compared with the Mock, the proliferative

activity of QC cells (Figure S26A~F) and QC-like cells (Figure S26A,B,D,F) in the 30 μM Bik are markedly increased (Figure S26A~F). EdU staining assays further demonstrated that the proliferative activity of QC cells (nondividing cells) and QC-like cells (more and wider nondividing cells) in the 30 μM Bik are markedly enhanced (Figure S26G~L). These findings suggest that a reduction in phosphorylated WOX5 protein levels can enhance the proliferative activity of cells. Finally, we processing genetic materials of QC25/*c3c4* and QC184/*c3c4* using 30 μM Bik and viewed root tips by GUS staining assays. Compared to the Mock, we observed a significant reduction in GUS activity of QC25 and QC184 in QC, SI, and SID when treated with 30 μM Bik (Figure S26M~X), suggesting that reduced phosphorylated WOX5 protein would lead to decreased GUS activity in these cells. All these results suggest that increased phosphorylated WOX5 protein is required for producing more quiescent cells and for increasing GUS activity of QC184 and QC25.

Cantharidin (CT), a potent inhibitor of the catalytic subunit (C subunit) of PP2A holoenzymes (Li and Casida, 1992), is utilized to further confirm that the essential role of WOX5 in promoting the production of quiescent cells and enhancing GUS activity in QC184 and QC25, by inhibiting the subfamily II of AtPP2A-Cs. Firstly, to determine the optimum concentration of CT and time for processing root tips, we transplant 4 DAG Col-0 seedlings to the ½ MS medium with 0 (DMSO, the Mock), 15 and 30 μM CT for 24 hours, and 48 hours (Bian et al., 2020). We found that only the 30 μM CT for 48 hours could appear the phenotypes of short root and more root hairs which are similar to the root phenotypes of *c3c4* mutant (Figure S27), rather than the Mock and 15 μM CT (Figure S27). Furthermore, 30 μM CT effectively impedes the dephosphorylation activity of both AtPP2A-C3-GFP and AtPP2A-C4-GFP in the reaction buffer. However, Lambda PP's dephosphorylation activity remains unaffected by the presence of CT (Figure 6W). So we next transplanted 4 DAG seedlings of Col-0 and *wox5-1* to the ½ MS medium with the Mock and 30 μM CT for 48 hours, then we viewed the SCN of root tips using improved mPS-PI staining. We noticed that the starch grains of all root tips of 30 μM CT for 48 hours disappeared or partly disappeared, also indicated that 30 μM CT for 48 hours could interface other pathways (like auxin distribution and/or gravitropism) by inhibiting the dephosphorylation activity of the AtPP2A-Cs (Ballesteros et al., 2013; Bian et al., 2020; Rahman et al., 2010). We observed that compare to the 100% one layer QC cells of the Mock (Figure S28A), 43.18% root tips of Col-0 in the 30 μM CT exhibited two layers QC-like cells (Figure S28B), 36.36% showed more and wider QC-like cells (Figure S28C), 20.45% displayed one layer QC cells (Figure S28D). However, the phenotype of *wox5-1* in 30 μM CT (90.24%), characterized by one layer high PA cells (Figure S28F), showed almost no difference from that in the Mock (93.75%) (Figure S28E). The EdU staining assays

showed that compared with 95.24% one layer nondividing cells of the Mock (Figure S28G), 44.83% root tips of Col-0 in the 30 μM CT were two layers nondividing cells (Figure S28H), 34.48% were more and wider nondividing cells (Figure S28I), 20.69% were one layer nondividing cells (Figure S28J). However, the phenotype (one layer dividing cells) of *wox5-1* in 30 μM CT (85.71%) (Figure S28L) was almost not different with in Mock (89.47%) (Figure S28K). The results indicate that inhibiting the function of the subfamily II of AtPP2A-Cs by CT can also produce more quiescent cells and WOX5 is required for it. Finally, we transplant 4 DAG seedlings of QC25, QC25/*wox5-1* and QC184 QC184/*wox5-1* to the ½ MS medium with the Mock and 30 μM CT for 48 hours. The GUS staining assay showed a significant increase GUS activity in the QC cells of QC25 treated with 30 μM CT compared to Mock (Figure S29A~D,G~J), and GUS activity of QC25 and QC184 appeared in the SI and SID (two layers blue cells and more and wider blue cells) in the 30 μM CT, not in the Mock (Figure S29A~D,G~J). However, there was no significant difference in GUS activity of QC25/*wox5-1* and QC184/*wox5-1* in 30 μM CT compared to the Mock (FigureS29E,F,K,L). These data suggest that WOX5 is necessary for increasing GUS activity of QC184 and QC25 when inhibiting the subfamily II of AtPP2A-Cs.

Taken together, all these results demonstrate that the subfamily II of AtPP2A-Cs regulates the homeostasis of QC, and WOX5 protein is required for it.

In situ overexpressed WOX5 protein recapitulated more quiescent cells

The results of Figure 7, Figure S24, Figure S28 and Figure S29 proved that WOX5 protein was required for producing more quiescent cells when loss of function of the subfamily II of AtPP2A-Cs, however, it is yet to be determined whether WOX5 protein simultaneously upregulated in QC, SI, and SID in WT causes production of more quiescent cells. Previous studies (Burkart et al., 2019; Pi et al., 2015) and our WOX5 transcriptional reporters (Figure S30A,B) have all showed that WOX5 mainly expressed in the QC cells and slightly expressed in the SI and SID. Thus, in order to obtain genetic material of WOX5 protein simultaneously upregulated in QC, SI, and SID (here we called in situ overexpressed WOX5 protein), we introduced the GVUAS:WOX5GFP plasmid into Col-0 and *wox5-1*, obtained transgenetic homozygous lines of GVUAS:WOX5GFP/Col-0 and GVUAS:WOX5GFP/*wox5-1*. Quantification of GFP intensity show that the WOX5GFP protein in QC, SI, and SID of GVUAS:WOX5GFP/Col-0 line is significantly higher than the pWOX5:WOX5GFP/Col-0 line (Figures S31A-E), and GVUAS:WOX5GFP/*wox5-1* line is also markedly higher than pWOX5:WOX5GFP/*wox5-1* line (Figure S31F-J), suggesting that WOX5 protein in situ overexpressed successfully.

Firstly, we viewed pWOX5:WOX5GFP lines and in situ overexpressed WOX5 protein lines by improved mPS-PI. Compared with the 100% one layer QC cells of root tips and mature embryos of pWOX5:WOX5GFP/Col-0 line, 58.93% root tips and 52.63% mature embryos of GVUAS:WOX5GFP/Col-0 line presented two layers QC-like cells (Figure S32B and S32F), 26.79% root tips and 26.32% mature embryos of GVUAS:WOX5GFP/Col-0 line appeared more and wider QC-like cells (Figure S32C and S32G), only 14.29% root tips and 21.05% mature embryos of GVUAS:WOX5GFP/Col-0 line kept one layer QC cells (Figure S32D and S32H). These data indicated that in situ overexpressed WOX5 protein in Col-0 could recapitulate the phenotypes of more QC-like cells in *c3c4* from the embryonic stage to the postembryonic stage. Likewise, compared with the 100% one layer QC cells of root tips and mature embryos of pWOX5:WOX5GFP/*wox5-1* line, 60.00% root tips and 54.00% mature embryos of GVUAS:WOX5GFP/*wox5-1* line presented two layers QC-like cells (Figure S33C and S33H), 30.00% root tips and 36.00% mature embryos of GVUAS:WOX5GFP/*wox5-1* line appeared more and wider QC-like cells (Figure S33D and S33I), and 10.00% root tips and 10.00% mature embryos of GVUAS:WOX5GFP/*wox5-1* line kept one layer QC cells (Figure S33E and S33J). These data indicated that in situ overexpressed WOX5 protein in *wox5-1* not only rescued the phenotypes of *wox5-1* (Figure S33A and S33F), but also recapitulated the phenotypes of more QC-like cells in *c3c4* from the embryonic stage to the postembryonic stage.

Secondly, EdU staining assays showed that compared with almost 91.67% one layer nondividing cells of root tips of pWOX5:WOX5GFP/Col-0 line, 54.17% root tips of GVUAS:WOX5GFP/Col-0 line presented two layers nondividing cells (Figure S32J), 30.56% appeared more and wider nondividing cells (Figure S32K), 15.28% kept one layer nondividing cells (Figure S32L). The data indicated that in situ overexpressed WOX5 protein in Col-0 could recapitulate the phenotypes of more nondividing cells in *c3c4*. Likewise, compared with almost 90.48% one layer nondividing cells of root tips of pWOX5:WOX5GFP/*wox5-1* line, 50.85% root tips of GVUAS:WOX5GFP/*wox5-1* line presented two layers nondividing cells (Figure S33M), 32.20% appeared more and wider nondividing cells (Figure S33N), 16.95% kept one layer nondividing cells (Figure S33O). The results suggest that in situ overexpressed WOX5 protein in *wox5-1* not only rescued the phenotypes of 100% one layer dividing cells of *wox5-1* (Figure S33K), but also recapitulated more nondividing cells in *c3c4*.

Thirdly, in order to further testify whether in situ overexpressed WOX5 protein can increase GUS activity of QC25 and QC184 in QC, SI, and SID. We combined QC markers (QC184 and QC25) with GVUAS:WOX5GFP/Col-0 line and GVUAS:WOX5GFP/*wox5-1* line for obtaining QC184/GVUAS:WOX5GFP/Col-0, QC184/GVUAS:WOX5GFP/*wox5-1* homozygous lines and

QC25/GVUAS:WOX5GFP/Col-0, QC25/WOX5GFP/*wox5-1* homozygous lines. Then we processed the 5 DAG root tips of these materials by GUS staining, compared with 100% one layer blue cells of QC184 (Figure S32M) and QC25 (Figure S32Q), 40.82% root tips of QC184/GVUAS:WOX5GFP/Col-0 line (Figure S32N) and 62.20% QC25/GVUAS:WOX5GFP/Col-0 line (Figure S32R) presented two layers blue cells, 44.90% root tips of QC184/GVUAS:WOX5GFP/Col-0 line (Figure S32O) and 17.78% QC25/GVUAS:WOX5GFP/Col-0 line (Figure S32S) appeared more and wider blue cells, only 14.29% root tips of QC184/GVUAS:WOX5GFP/Col-0 line (Figure S32P) and 20.00% QC25/GVUAS:WOX5GFP/Col-0 line (Figure S32T) kept one layer blue cells. The result show that the GUS activity in QC of all these materials are markedly higher than QC184 (Figure S32M-P) and QC25 (Figure S32Q-T), and the GUS activity in SI and SID appeared in most of these materials (Figure S32N-P and S32R-T), but not in QC184 (Figure S32M) and QC25 (Figure S32Q). Likewise, compared with 100% one layer blue cells of QC184 (Figure S33Q) and QC25 (Figure S33V), 37.04% root tips of QC184/GVUAS:WOX5GFP/*wox5-1* line (Figure S33R) and 51.43% QC25/GVUAS:WOX5GFP/ *wox5-1* line (Figure S33W) presented two layers blue cells, 48.15% root tips of QC184/GVUAS:WOX5GFP/*wox5-1* line (Figure S33S) and 31.43% QC25/GVUAS:WOX5GFP/*wox5-1* line (Figure S33X) appeared more and wider blue cells, only 14.81% root tips of QC184/GVUAS:WOX5GFP/*wox5-1* line (Figure S33T) and 17.14% QC25/GVUAS:WOX5GFP/*wox5-1* line (Figure S33Y) kept one layer blue cells. The results showed in situ overexpressed WOX5 protein not only rescue the phenotypes of one layer not blue cells of QC184/*wox5-1* (Figure S33P) and one layer light blue cells of QC25/*wox5-1* (Figure S33U), but also increased GUS activity in QC, SI, and SID (Figure S33Q-T and Figure S33V-Y). All these data indicated that increased WOX5 protein in SI and SID is sufficient for reducing the proliferative activity of QC and enhancing GUS activity of QC184/QC25, and increased WOX5 protein in QC is also sufficient for reducing the proliferative activity of QC and increasing GUS activity of QC184/QC25.

Finally, in order to view directly increased WOX5 protein in QC cause its PA reduction and increased WOX5 protein in SI and SID lead to these cells convert to QC-like cells. We introduced the GVUAS:GR-WOX5GFP plasmid into *wox5-1*, obtained transgenetic homozygous lines of GVUAS:GR-WOX5GFP/*wox5-1*. For observing the process of dynamic accumulation of WOX5GFP protein, we plant seeds of lines of GVUAS:GR-WOX5GFP/*wox5-1* into ½ MS medium with 20 μM Dexamethasone (Dex) and the Mock with DMSO. We viewed lots of root tips at selected 5 time nodes (3.0 days, 3.5 days, 4.0 days, 4.5 days, 5.0 days) separately. Through the GFP imaging and PI staining assays and EdU staining assays, we found that in the Mock (no

induction), the GR-WOX5GFP protein could not rescue the phenotypes of one layer high PA cells of *wox5-1* (100.00%) (Figure S34A and S34G) and one layer dividing cells (100.00%) (Figure S34M). But the dynamic accumulation of WOX5GFP protein in QC at 3.0 DAG after induction (20 μM Dex) causes one layer QC cells with WOX5GFP protein (90.91%) (Figure S34B and S34H) and one layer nondividing cells (91.67%) (Figure S34N). The dynamic accumulation of WOX5GFP protein in SI from 3.0 DAG to 4.5 DAG after induction leads to the dividing SI cells (91.67%, 81.48%) (Figure S34N and S34O) with low content WOX5GFP protein (90.91%, 91.30%) (Figure S34B,C,H,I) gradually convert to nondividing one layer QC-like cells (65.51%, 50.00%) (Figure S34P,Q) with high content WOX5GFP protein (88.88%, 62.50%) (Figure S34D,E,J,K). The dynamic accumulation of WOX5GFP protein in SID from 4.5 DAG to 5.0 DAG after induction leads to dividing SID cells (50.00%) (Figure S34Q) with low content WOX5GFP protein (62.50%) (Figure S34E,K) convert to nondividing one layer QC-like cells (50.00%) (Figure S34R) with high content WOX5GFP protein (50.00%) (Figure S34F,L). These data suggest that increased WOX5 protein in QC causes its PA reduction and increased WOX5 protein in SI and SID lead to PA reduction of these cells.

Taken together, in situ overexpressed WOX5 protein is sufficient for producing more quiescent cells.

Phosphate-mimicked WOX5 protein partially recapitulated more quiescent cells

To confirm the critical role of phosphorylated WOX5 protein in its stability and reduction of PA of SI and SID. Firstly, we noticed that some phosphate-mimicked homozygous lines (WOX5m3D-GFP/*atsk21/22/23* line #2 and WOX5m5D-GFP/*atsk21/22/23* line #1, line #22) recapitulated the phenotype of two layers QC-like cells in *c3c4* from the embryonic stage to the postembryonic stage (Figure S35B~D and S35G~I), but WOX5GFP/*atsk21/22/23* lines not appeared the phenotype of two layers QC-like cells (Figure S35A and S35F). Meanwhile, compare with WOX5 protein, phosphate-mimicked WOX5 protein not only increased in QC (Figure 4G~J), but also increased in SI and SID (Figure S35E). The results indicate that although without kinase activity of the subfamily II of AtSKs, phosphate-mimicked WOX5 protein can't be dephosphorylated by AtPP2A-Cs holoenzymes, therefore, the WOX5 protein remains continuously phosphorylated and stabilized, leading to the conversion of SI and SID cells into QC-like cells. Secondly, we introduced WOX5m3D-GFP and WOX5m5D-GFP driving by the full-length promotor plus 5' untranslated region (UTR) and 3'UTR of WOX5 genomic sequence (Figure S2) into Col-0, obtained WOX5m3D-GFP/Col-0 and WOX5m5D-GFP/Col-0 homozygous lines. We found that phosphate-mimicked WOX5 protein of WOX5m3D-GFP/Col-0

line #2 and WOX5m5D-GFP/Col-0 line #1 markedly increased in QC, SI, and SID (Figure S36B-D) when compared with WOX5 protein of WOX5GFP/Col-0 line (Figure S36A and S36D), suggesting that phosphate-mimicked WOX5 protein is more stable than WOX5 protein. Thus, we speculate that the more stable phosphate-mimicked WOX5 protein will cause the PA reduction of SI and SID. The improved mPS-PI staining showed that 38.30% root tips (Figure S37B) and 37.84% mature embryos (Figure S37E) of WOX5m3D-GFP/Col-0 line #2, 41.67% root tips (Figure S37C) and 39.47% mature embryos (Figure S37F) of WOX5m5D-GFP/Col-0 line #1 presented two layers QC-like cells, but 100% root tips (Figure S37A) and 100% mature embryos (Figure S37D) of WOX5GFP/Col-0 line were one layer QC cells. The EdU staining assays showed that 41.18% root tips (Figure S37H) of WOX5m3D-GFP/Col-0 line #2 and 45.45% root tips (Figure S37I) of WOX5m5D-GFP/Col-0 line #1 appeared two layers nondividing cells, but 88.00% root tips (Figure S37G) of WOX5GFP/Col-0 line were one layer nondividing cells. These data suggest that phosphate-mimicked WOX5 protein stabilizes itself and reduces PA of SI and SID, thus produces more quiescent cells. To further confirm that whether stabilized phosphorylated WOX5 protein can enhance GUS activity of QC184 in QC, SI, and SID. We introduced WOX5m3D-GFP driving by the full-length promotor plus 5' untranslated region (UTR) and 3'UTR of WOX5 genomic sequence (Figure S2) into QC184/*wox5-1*, then obtaining WOX5m3D-GFP/QC184/*wox5-1* homozygous lines. The GUS staining assays showed that 44.44% root tips of WOX5m3D-GFP/QC184/*wox5-1* line appeared two blue cells (Figure S37L), not only rescued the phenotypes of not blue cells of QC184/*wox5-1* (Figure S37J), but also simultaneously enhanced the GUS activity in QC and SI when compared with the GUS activity of WOX5GFP/QC184/*wox5-1* rescued line (Figure S37K). The results demonstrated that stabilized phosphorylated WOX5 protein can enhance GUS activity of QC184 in QC and SI. Owing to the subfamily II of AtSKs stabilizes WOX5 protein by phosphorylating the GMs (Figure S19), and the 30 μM Bik can destabilize WOX5-GFP protein by inhibiting the activity of the subfamily II of AtSKs (Figure S16C~D and S16F). Thus, we want to figure out whether the 30 μM Bik can destabilize the phosphate-mimicked WOX5 protein. Finally, we planted the WOX5m3D-GFP/Col-0 line and WOX5m5D-GFP/Col-0 line in the 30 μM Bik and the Mock for 5 days. We observed root tips and counted the PA of QC and quantified the fluorescence of GFP intensity in QC, SI, and SID. The results showed that there were no significant differences in QC, SI and SID between 30 μM Bik and the Mock (Figure S38A-I), meanwhile, the PAr of QC in 30 μM Bik was not different with the Mock (Figure S38J), suggesting that inhibiting the kinase activity of the subfamily II of AtSKs by using 30 μM Bik, phosphate-mimicked WOX5 protein still stabilize itself in QC, SI, and SID, and chemical inhibiting the activity of the subfamily II of AtSKs can't

either destabilize the continuous phosphorylated phosphate-mimicked WOX5 protein (WOX5m3D-GFP and WOX5m5D-GFP), nor increase the PAr of QC. We further viewed root tips using EdU staining, the percentage of one layer nondividing cells at 30 μM Bik was not significantly different between the WOX5m3D-GFP/Col-0 line (48.48%) and the WOX5m5D-GFP/Col-0 line (53.13%), compared to the Mock (50.00% and 51.61% respectively) (Figure S38K-L and S38O-P). Similarly, the percentage of two layers nondividing cells at 30 μM Bik was also not significantly different between the WOX5m3D-GFP/Col-0 line (42.42%) and the WOX5m5D-GFP/Col-0 line (40.63%), compared to the Mock (40.63% and 45.15% respectively) (Figure S38M-N and S38Q-R), suggesting that chemical inhibiting the activity of the subfamily II of AtSKs could not increase the proliferative activity of the more quiescent cells which produced by stabilized phosphate-mimicked WOX5 protein in SI and SID, too. In addition, we planted the WOX5m3D-GFP/QC184/*wox5-1* line in the 30 μM Bik and the Mock for 5 days. The GUS staining assays showed that the one layer blue cells of 30 μM Bik (45.76%) was not different with the Mock (46.81%) (Figure S38S-T), and the two layers nondividing cells of 30 μM Bik (54.24%) was also not different with the Mock (53.19%) (Figure S38U-V), suggesting that inhibiting the kinase activity of the subfamily II of AtSKs by using 30 μM Bik, WOX5 protein can't maintain the activity of QC184 GUS activity in QC (Figure S14A and S14E), but phosphate-mimicked WOX5 protein still enhanced the activity of QC184 GUS activity not only in QC but also in SI and SID. Taken together, phosphate-mimicked WOX5 protein is sufficient for producing more quiescent cells.

Conclusion

WOX5 protein is phosphorylated by the subfamily II of AtSKs and dephosphorylated by the subfamily II of AtPP2A-Cs holoenzymes, the homeostasis of WOX5 protein is regulated by reversible phosphorylation, which make sure the homeostasis of low proliferative activity of QC cells. In addition, the subfamily II of AtPP2A-Cs increase the proliferative activity of SI and SID by down-regulating WOX5 expression and reducing stability of WOX5 protein, which determine the homeostasis of one layer QC cells.

Discussion

It is widely known that the WOX5 protein expresses in the QC cells and maintains their quiescence from the embryonic stage to the postembryonic stage (Celine et al., 2014; Haecker et al., 2004). However, QC cells are not in a strictly quiescent state (G0 stage) but in a resting state (G1 stage) with very low proliferative activity, these resting QC cells can re-enter the cell cycle

when needed (Clowes, 1968; Matosevich and Efroni, 2021; Ubogoeva et al., 2021). How accurately define the low proliferative activity of QC is unclear. Here, we define the phenotype of QC proliferative activity by a novel Proliferative Activity (PA) index, and we find that the dynamic balance of phosphorylated WOX5 protein maintains the dynamic balance of low PA of QC. On one hand, the subfamily II of AtSKs phosphorylate WOX5 protein and stabilize WOX5 protein, thereby inhibiting the proliferative activity of QC cells and establishing quiescence. Consequently, no phosphorylation sites of WOX5 protein (truncation of PEST domain and all types of serine/threonine (S/T) to alanine (A) site-directed mutagenesis) and no kinase activity (loss of function mutant of the subfamily II of AtSKs and treatment with 30 μM Bik) will reduce WOX5 protein and increase PA of QC (Figure S39C,F). On the other hand, the subfamily II of AtPP2A-Cs holoenzymes (may act as a molecular switch) dephosphorylate the phosphorylated WOX5 protein and promote its degradation. This mechanism facilitates proliferation in QC cells when required, as demonstrated by the increased PA of QC cells upon overexpression of the subfamily II of AtPP2A-Cs holoenzymes (Figure S39F). In addition, why constantly exist just one layer QC with low proliferative activity at the centre of RAM in *Arabidopsis* from the embryonic stage to the postembryonic stage remains elusive. Our solid genetic proofs including no phosphotase activity (loss-of-function mutations in the subfamily II of AtPP2A-Cs and treatment with 30 μM CT), phosphate-mimicked WOX5 protein (all types of serine/threonine (S/T) to asparticacid (D) site-directed mutagenesis), and in situ overexpressed WOX5 protein will increase WOX5 protein in QC, SI, and SID and reduce PA of QC, SI, and SID. Consequently, this causes the emergence of two layers QC-like cells and more and wider QC-like cells (Figure S39E,H). Moreover, dynamic accumulation of WOX5 protein directly converts the SI and SID into QC-like cells. This is the first discovery reveals that active stem cells can convert into quiescent stem cells in plants (Li and Clevers, 2010). As a result, the subfamily II of AtPP2A-Cs enhance the proliferative activity of SI and SID by down-regulating WOX5 expression and reducing stability of WOX5 protein, thus maintaining the balance of one layer QC (Figure S39B).

To clarify the relationship between QC PA and QC identity, we use two promotor trapping lines of QC25 and QC184 as QC identity markers (Brand and Perrimon, 1993). No phosphorylation sites of WOX5 protein can’t completely rescue the GUS activity of QC184, and no kinase activity downregulates the GUS activity of QC184 and QC25 (Figure S7). Our findings suggest a reciprocal relationship between WOX5 protein level, the PA of QC cells, and QC identity. Specifically, a reduction in WOX5 protein levels enhances the PA of QC cells, while an increase in WOX5 protein levels reduces QC PA and strengthens QC identity. Contrarily, no phosphotase activity, phosphate-mimicked WOX5 protein, and in situ overexpressed WOX5 protein not only upregulate the GUS activity of QC184 and QC25 in QC, but also increase the GUS activity of QC184 and QC25 in SI and SID (Figure S29). This suggests that increased WOX5 protein levels in QC can reduce QC PA and enhance QC identity. In contrast, increased WOX5 protein levels in SI and SID can reduce PA of SI and SID cells leading to a reduction in their PA, resulting in their conversion to QC-like cells and acquisition of QC identity. In a word, our results highlight that a decrease in QC PA enhances QC identity, whereas the increased QC PA will weaken QC identity.

Reversible phosphorylation is one of the most common and crucial mode of post-translational modifications for regulating protein stability and/or activity, thus mediating various cell signal transduction pathways (Ardito et al., 2017). Phosphorylated by protein kinases and

dephosphorylated by protein phosphatases, these pairs of phosphate group antagonists are widely widespread in animals and plants (Tan et al., 2021; Worby and Dixon, 2019). In mammals, a well-known pair of antagonist, glycogen synthase kinase 3 (GSK3) and protein phosphatase 2A (PP2A), was involved in regulating the homeostasis of β-catenin transcriptional coactivator in Wnt signaling pathway, thereby modulates cell fate determination and stem cell pluripotency maintenance (MacDonald et al., 2009). Likewise, in *Arabidopsis*, BR-INSENSITIVE 2 (BIN2) (a homolog of GSK3) and PP2A oppositely regulate the key transcriptional factor BZR1 of brassinosteroid signalling (Di Rubbo et al., 2011; He et al., 2002; Tang et al., 2011) and critical transcriptional factors AKSs (ABA-responsive kinase substrates) of ABA signalling (Bu et al., 2017), thereby modulateing root growth and development, stem cell self-renewal and stress adaption (Chen et al., 2020; Planas-Riverola et al., 2019). However, whether the antagonist pair (GSK3 and PP2A) directly regulates the central transcriptional factor WOX5 in the root stem cell niche remains unknown. In this study, we firstly find that WOX5 protein is modified by reversible phosphorylation, which controls the homeostasis of QC. The subfamily II of AtSKs (the homologs of GSK3 in *Arabidopsis*) stabilize WOX5 protein by phosphorylating the GSK3 motifs (GMs) in PEST domain, and the subfamily II of AtPP2A-Cs holoenzymes destabilize WOX5 protein by dephosphorylating the phosphorylated GMs (Figure S39A). Remarkably, the regulatory mechanism of WOX5's stability is contrary to the β-catenin protein and BZR1 protein mediating by GSK3 and PP2A (Di Rubbo et al., 2011; MacDonald et al., 2009), but is consistent with other proteins and comports with the dual roles of phosphorylation of GSK3 (Hu and Yu, 2014; Yamamoto et al., 1999; Ye et al., 2012). In order to investigate whether the WOX5 protein homeostasis is regulated by post-translational modifications, we analyzed the WOX5 protein sequence and uncovered a signal peptide, called PEST domain, that contributes to protein degradation (Belizario et al., 2008; Rechsteiner and Rogers, 1996; Rogers et al., 1986). However, our solid genetic and biochemical proofs testify that the PEST domain is accessible for phosphorylation and dephosphorylation, thus controlling the homeostasis of WOX5 protein. These results suggest that the conformational flexible PEST domain may play multiple roles in regulating protein homeostasis (Sandhu and Dash, 2006).

In conclusion, our findings answered two fundamental questions of why *Arabidopsis* always exists just one-layer QC cells and how these one-layer QC cells always maintain low proliferative activity (Figure S39B,D,G). In addition, the subfamily II of AtPP2A-Cs increase the proliferative activity of SI and SID by down-regulating WOX5's expression and reducing stability of WOX5 protein, which determine the homeostasis of one layer QC cells (Figure S39B,D,G).

EXPERIMENTAL MODEL AND SUBJECT DETAILS

Plant growth conditions

Arabidopsis thaliana plants were grown in nutrient soil and vermiculite (2:1) inside growth cabinets held at 22℃ and 55% humidity with a 16/8 hours photoperiod (130 $\mu mol.m^{-2}.s^{-1}$). *Nicotiana benthamiana* plants were grown in nutrient soil and vermiculite (2:1) inside chambers held at 25℃ and 65% with a 14/10 hours photoperiod (130 $mmol.m^{-2}.s^{-1}$).

In this study, seeds were stratified for 48-72 hours at 4°C in darkness to break dormancy before planted onto the ½ MS medium. ½ MS medium refers to Murashige and Skoog medium with the following recipe: 0.5× Murashige & Skoog MEDIUM including Vitamins (Duchefa Biochemie) and 0.5% (w/v) MES (Sangon Biotech (shanghai) Co.,Ltd.) at a pH of 5.7 supplemented with 1% agar (SERVA high gel strength) and 1% sucrose (Sigma-Aldrich).

Transgenic plant lines

Transgenic plant lines were generated by *Agrobacterium tumefaciens*-mediated (GV3101 strain with a Tetracyclin-resistant pSoup plasmid) floral dip transformation. Transgenic seedlings (T_1) were selected in ½ MS medium with 1 μM Norflurazon (Norf) (Sigma-Aldrich) and 0.8% agar (SERVA high gel strength) and without sucrose, all T_1 seedlings were transplanted on ½ MS medium with 50 μg/mL Ampicillin (Amp) and 1% agar (SERVA high gel strength) and without sucrose. Seeds of each T_2 line that were harvested from each T_1 line was planted onto ½ MS medium with 1 μM Norflurazon (Norf), homozygote T_3 lines (the seeds of Norf-resistant T_2 lines) were then identified by verifying that all T_3 seedlings were Norf-resistant.

Arabidopsis mutant

In this study, the T-DNA mutant lines of *wox5-1*, *atsk21/22/23* and *c3c4* were obtained from Limin Pi lab (Pi et al., 2015; Sarkar et al., 2007), Xuelu Wang lab (Yan et al., 2009), and Martine Pastuglia lab (Spinner et al., 2013) under the background of Col-0, Wassilewskija (Ws), and Col-0 ecotype respectively.

METHOD DETAILS

Plasmid construction for *Arabidopsis* experiments

All plasmids (Table S1) for transformating *Arabidopsis* were generated from the NK43 vector, all promotor sequences were amplified with primers (Table S1) by Phanta Max Super-Fidelity DNA Polymerase (Nanjing Vazyme Biotech Co.,Ltd.) PCR from Col-0 DNA extracted by CTAB method, all coding sequences were amplified by Phanta Max Super-Fidelity DNA Polymerase (Nanjing Vazyme Biotech Co.,Ltd.) PCR from cDNA (see sqRT-PCR and qPCR assays), all these fragments were cloned into NK43 vector by using In Fusion Cloning (ClonExpress® II One Step Cloning Kit, Nanjing Vazyme Biotech Co.,Ltd.) and/or Restriction Cloning (FastDigest Restriction enzymes and T4 DNA ligase kit, Thermo Fisher Scientific).

Site-directed mutagenesis

In order to change and/or delete some specific amino acids sites of proteins, site-directed mutagenesis of CDS sequences of WOX5 and AtSK21 using In Fusion Cloning with special primers (Table S2). Successful mutagenesis of CDS sequences of WOX5mGM1, WOX5mGM2, WOX5ΔPEST, WOX5mAll, WOX5m5A, WOX5m3A, WOX5m3D, WOX5m5D, and AtSK21(K69R) were convinced by DNA sequencing (Tsingke Biotechnology Co., Ltd.).

sqRT-PCR and qPCR assays

According to manufacturer's instructions, DNA-free total RNA was extracted from 50-100 mg root tips (almost 1 cm length) of 5DAG seedlings by using FastPure® Plant Total RNA Isolation Kit (Nanjing Vazyme Biotech Co.,Ltd.), cDNA was synthesized from extracted RNA (measured by Thermo Fisher Scientific Nanodrop One^{C}) by using HiScript® III 1st Strand cDNA Synthesis Kit (+gDNA wiper) (Nanjing Vazyme Biotech Co.,Ltd.), sqRT-PCR was performed by using Green Taq Mix (Nanjing Vazyme Biotech Co.,Ltd.), qPCR was performed by using ChamQ SYBR Color qPCR Master Mix (Nanjing Vazyme Biotech Co.,Ltd.). A sqRT-PCR primer pair GFPlinkF and GFPtaaR were used to quantify expression level of GFP-fused protein (Table S3), sqRT-PCR primer pairs gene-RT-Fs and gene-RT-Rs were used to quantify expression level of genes (Table S3), a primer pair ACT2-RT-F and ACT2-RT-R were used to quantify expression level of ACT2 (AT3G18780, the reference gene) (Table S3). A qPCR primer pair GFP111aaF and GFP162aaR were used to quantify expression level of GFP-fused protein, WOX5-RT-F and WOX5-RT-R were used to quantify expression level of WOX5 protein (Table S3), the reference gene was used to normalize gene expression levels, reactions of qPCR were run on the CFX Touch 96-well Real-Time PCR Detection Systems and were repeated three times.

GFP imaging and PI staining

Root tips of GFP fused protein transformed *Arabidopsis* were transferred onto slides and covered with a drop of 100 times diluted Propidium Iodide (PI) solution (1.0 mg/mL) (Sigma-Aldrich) for one minute, a coverslip was placed on top before the observation. All samples were imaged on the LEICA TCS SP8 laser scanning confocal microscope with the HCX PL APO 40×/0.85 DRY objective, GFP and PI fluorescence signals were detected by exciting with laser at 488nm and 552 nm, and by collecting emission from 500-520 nm and 600-650 nm on a HyD detector and a PMT detector at the sequential scan mode. All images were acquired by using the Leica Application Suite X software 3.5.2.18963. All pWOX5:WOX5GFP fluorescence and pWOX5:nlsGFP samples that were compared in the publication were imaged with the same laser intensity 35.0 of 488 nm (accumulation twice) and 10.0 of 488nm (not accumulation), respectively.

Improved mPS-PI staining

We improved the mPS-PI staining method (Truernit et al., 2008), as described below. Root tips and mature embryos of *Arabidopsis* were fixed in solution I (50% methanol and 10% acetic acid) at 4°C for at least 12 h. Next, samples were rinsed with water twice and incubated in solution II [1% (w/v) periodic acid] at room temperature for 1 hour. Samples were rinsed again with water twice, then, incubated in solution III (Schiff reagent, 100 mM sodium metabisulphite and 0.15 N HCl) with propidium iodide (a final concentration of 10 μg/mL) freshly added for 5 min. The samples were transferred onto slides and covered with a drop of chloral hydrate solution (4 g chloral hydrate, 1 mL glycerol, and 2 mL water), a coverslip was placed on top before observation. All samples were imaged by the LEICA TCS SP8 laser scanning confocal microscope with the HCX PL APO 40×/0.85 DRY objective, propidium iodide fluorescence signal were detected by exciting with a laser at 552 nm, and by collecting emission from 600-650 nm on two PMT detectors. All images were acquired by using the Leica Application Suite X software 3.5.2.18963.

BiFC in *Tobacco*

For BiFC assays, full-length CDS of *Arabidopsis* WOX5, AtSK21, AtSK22, AtSK23, AtPP2A-C3, AtPP2A-C4, HAM4, RGA were amplified with primers (Table S3) by Phanta Max Super-Fidelity DNA Polymerase (Nanjing Vazyme Biotech Co.,Ltd.) PCR from cDNA (see sqRT-PCR and qPCR assays), and recombined into vectors containing each half of YFP (N or C terminus) (Walter et al., 2004) to generate all needed plasmids (Table S4) with primers (Table S4) by using restriction cloning. *Agrobacterium tumefaciens* cultures (GV3101 strain) carrying the plasmid pairs for testing the specific interactions (p35S:WOX5-YFPN and p35S:CDS-YFPC) together with the p35S:nlsCFP (as a nuclear marker) plasmid (Table S4) were grown overnight at 28°C in liquid LB broth containing 50 μg/mL kanamycin (Sigma-Aldrich), 25 μg/mL gentamicin (Sigma-Aldrich), and 10 μg/mL rifampicin (Sigma-Aldrich). Cultures were centrifugated and the sediments were mixed with infiltration buffer (10 mM $MgCl_2$ (Sigma-Aldrich), 10 mM MES (Sangon Biotech (shanghai) Co.,Ltd.), and 150 μM acetosyringone (Sigma-Aldrich) at a pH of 5.6 and diluted to reach an OD600 of 1.0. Equal amount of each diluted culture was pre-mixed, fully expanded 3rd or 4th leaves from 4/5-week-old *Nicotiana benthamiana* plants were infiltrated with these pre-mixed cultures. The infiltrated *Nicotiana benthamiana* plants were moved into darkroom at 22°C and 55% humidity for 12 hours, then were moved into lightroom of 14/10 hours photoperiod (130 $mmol.m^{-2}.s^{-1}$) for 2 or 3 days. The infiltrated tobacco leaves were imaged using a LEICA TCS SP8 laser scanning confocal microscope with the HCX PL APO 40×/0.85 DRY objective. CFP, YFP fluorescence signals and bright field (BF) were detected by exciting with laser at 448nm and 514 nm, and by collecting emission from 465-485 nm and 525-540 nm on two PMT detector and a TLD detector (514 nm PMT trans) at the sequential scan mode. All images were acquired by using the Leica Application Suite X software 3.5.2.18963.

Yeast Two Hybrid (Y2H)

For Y2H assays, full-length CDS of *Arabidopsis* WOX5, TPR1, AtSK11, AtSK12, AtSK13, AtSK21, AtSK22, AtSK23, AtSK31, AtSK32, AtSK41, AtSK42, AtPP2A-C1, AtPP2A-C2, AtPP2A-C3, AtPP2A-C4, AtPP2A-C5 were amplified by Phanta Max Super-Fidelity DNA Polymerase (Nanjing Vazyme Biotech Co.,Ltd.) PCR from cDNA (see sqRT-PCR and qPCR assays), and recombined into the vector pGADT7 and/or the vector pGBKT7 to generate all needed plasmids (Table S5) with primers (Table S5) by using Restriction cloning and In Fusion cloning. Plasmid pairs for testing the specific interactions were co-transformed into the yeast strain AH109. The yeast transformants were grown on nutrient-restricted (without Trp, Leu, His, Ade) mediums (Clontech) 3-5 days to assess interactions between various protein combinations.

Recombinant protein expression and purification

All plasmids (Table S6) for recombinant protein expression were generated from the vector pGEX-4T-1 and modified vector pGEX(MBP)-4T-1, recombinant protein expression using E. coli (BL21 strain) were performed according to the GST Gene Fusion System Handbook (GE healthcare Life Sciences). Recombinant GST-tagged proteins purification were performed according to the manufacturer's instructions of Pierce^{TM} Glutathione Superflow Agarose (Thermo Fisher Scientific), and recombinant MBP-tagged proteins purification were performed according to the manufacturer's instructions of Amylose Resin (NEB).

Pull-down in vitro Assays

For the pull-down in vitro assays, equal amount GST/GST-tagged input proteins, and MBP/MBP-tagged input proteins, and 30 μL MBP beads (Amylose Resin) were incubated in the 1 mL PL buffer [50 mM HEPES (pH=7.5), 150 mM NaCl, 1.5 mM MgCl2, 1 mM EGTA (pH=7.5), 1% Triton X-100, 5% Glycerol, 1 mM PMSF (Sigma Aldrich), 1× Protease Inhibitor Cocktail (EDTA-Free, 100X in DMSO) (bimake.cn)] for 1-2 hours at 4°C with gentle shaking. Then, the MBP beads were collected and washed with the PL buffer three times to eliminate nonspecific bindings. The beads of the pull-down proteins were analyzed by Western Blot with the Anti-MBP Tag (2A9) Monoclonal Antibody (1:5000) Produce in Mouse (GNI). Inputs were analyzed by Western Blot with Anti-MBP Tag (2A9) Monoclonal Antibody (1:5000) Produce in Mouse (GNI) and Mouse anti GST-tag mAb (1:2500, Abclonal).

Co-Immunoprecipitation (Co-IP) assays

For the Co-IP assays, 0.5-1.0 g root tips of 5 DAG seedlings of homozygous lines (p35S:LhGR-pOp:WOX5-YFP/Col-0, p35S:Flag-AtSK21/Col-0, p35S:Flag-C3/Col-0, p35S:Flag-C4/Col-0) and double homozygous lines (p35S:LhGR-pOp:WOX5-YFP×p35S:FlagAtSK21, p35S:LhGR-pOp:WOX5-YFP×p35S:FlagC3, p35S:LhGR-pOp:WOX5-YFP×p35S:FlagC4) were ground into powder in liquid nitrogen and homogenized in 0.5-1.0 mL cold IP buffer [50 mM Tris-HCl (pH =7.4), 150 mM NaCl, 1 mM $MgCl_2$, 20% Glycerol, 0.2% NP40, 1× Protease Inhibitor Cocktail] by gentle shaking or pipetting. Supernatants were incubated with anti-GFP beads for 4 h at 4°C with gentle shaking and washed 4 times with the IP buffer. Proteins of the Co-IP were analyzed by Western Blot with the Monoclonal ANTI-FALG® M2 antibody produced in mouse (Sigma Aldrich), proteins of inputs were analyzed by Western Blot with the Anti-GFP from mouse (Roche) and Monoclonal ANTI-FALG® M2 antibody produced in mouse (Sigma Aldrich).

Kinase assays

For kinase assays, kinase protein (GST-AtSK21), kinase-dead protein (GST-AtSK21K69R) and substrate proteins (MBP, MBPWOX5, MBPWOX5ΔPEST, MBPWOX5mAll, MBPWOX5m5A, MBPWOX5m3A) were generated by recombinant protein expression and purification. The kinase reaction (the amount of substrate was 2-5 times of kinase) was performed in 50 μL kinase buffer [25 mM Tris-HCl (pH=7.5), 10 mM $MgCl_2$, 1 mM ATP (Sigma Aldrich), 2 mM DTT] containing or not containing 30 μM Bik (Sigma Aldrich) at 30°C for 30-120 min, and then were incubated with 16 μL 4x loading buffer at 95°C for 10 minutes. The samples were sepereated by 8% SDS-PAGE gel containing 50 μM Mn^{2+}- Phos-tag™ (see Mn^{2+}-Phos-tag™ SDS-PAGE assays) and were analyzed by Western Blot with with the Anti-MBP Tag (2A9) Monoclonal Antibody (1:5000) Produce in Mouse (GNI).

Dephosphorylation assays

For dephosphorylation assays, the Protein Phosphatase 2A holoenzymes of C3GFP and C4GFP were extracted using lysis buffer [200 mM NaCl, 0.5% NP-40, 20 mM Tris-HCl (pH 8.0), 1x 1× Protease Inhibitor Cocktail and 1 mM PMSF (Sigma Aldrich)] and puried using anti-GFP beads from the total protein of root tips of homozygote p35S:C3GFP/Col-0 and p35S:C4GFP/Col-0 lines, and Lambda Protein Phosphatase (Lambda PP) was purchased from NEB. After kinase reaction in kinase buffer, 30 μM Bik was added in the kinase buffer for 1 h, and then added

overdose of phosphatase for 60-120 min, and then were incubated with 4x loading buffer at 95°C for 10 minutes. The samples were separated by 8% SDS-PAGE gel containing 50 μM Mn^{2+}-Phos-tag™ (see Mn^{2+}-Phos-tag™ SDS-PAGE assays) and were analyzed by Western Blot with with the Anti-MBP Tag (2A9) Monoclonal Antibody (1:5000) Produce in Mouse (GNI).

Mn^{2+}-Phos-tag™ SDS-PAGE

According to the Phos-tag™ SDS-PAGE guidebook (Wako), we selected the optium concentration of Mn^{2+}-Phos-tag™ (50 μM) and acrylamide (8%) for the separation of phosphorylated MBP-tagged substrates. After migrating with a constant voltage of 100 V in cold Tris-glycine-SDS (TGS) running buffer [25 mM Tris, 192 mM glycine, 0.1% SDS (w/v), pH 8.3] for 4 hours, and then transferred to Immobilon®-P^{SQ} Transfer Membrane (0.2 μm, Merck Millipore Ltd.) in 1x transfer buffer [25 mM Tris-HCl (pH 8.3), 192 mM glycine, 20% methanol (v/v)] containing 0.1% SDS (w/v) using a Bio-Rad transfer apparatus, and then were analyzed by Western Blot.

Western blot

For immunoblotting, samples were lysed in cold IP buffer (see pull-down assays) or IP buffer (see CoIP assays) or lysis buffer (see Dephosphorylation assays) mixed with 4x loading buffer [8% SDS (w/v), 40% glycerol, 4% β-mercaptoethanol, 0.008% bromophenol blue, 0.25 M Tris-HCl (pH=6.8)], and then boiled for 10 min. Subsequently, the samples were loaded in SDS-PAGE and transferred to Immobilon®-P^{SQ} Transfer Membrane (0.2 μM, Merck Millipore Ltd.) in 1x transfer buffer using a Bio-Rad transfer apparatus. The membrane was blocked with 5% non-fat milk in TBST [TBS buffer (50 mM Tris-Cl, pH 7.6; 150 mM NaCl) containing 0.1% (v/v) Tween-20] at room temperature for 30 min while shaking, followed by incubation with primary antibody overnight at 4°C while shaking. After three 10 min washes with TBST, membranes were incubated with species-specific secondary antibodies at room temperature for 1 h while shaking. Following three 10 min washes in TBST, the membrane was detected by enhanced chemiluminescent (ECL) substrate (ECL Substrate A, Peroxide Solution B, Vazyme Code: E412-01) and imaged with ChemDoc™ XRS+ with Image Lab™ Software (Bio-rad).

Chemical inhibitors assays

For the kinase inhibitor assays in vivo, seeds were planted in the ½ MS medium containing 30 μM Bik (Sigma Aldrich) for 6 days, for the kinase inhibitor assays in vitro, 30 μM Bik were added in the kinase buffer. For the Protein Phosphatase 2A holoenzymes inhibitor assays in vivo, seeds were planted in the ½ MS medium for 4 days and were transferred to the ½ MS medium containing 30 μM CT (Sigma Aldrich) for 48 hours, for the Protein Phosphatase 2A holoenzymes inhibitor assays in vitro, 30 μM CT were added in the kinase buffer.

GUS staining

The excised root tips of "QC25 marker line and its relevant genetic materials" and "QC184 marker line and its relevant genetic materials" were incubated in GUS staining solution (0.2% Triton X-100, 2□mM 5-bromo-4-chloro-3-indolyl glucuronide, 2□mM $K_3Fe(CN)_6$, 2□mM $K_4Fe(CN)_6$, 50 mM $NaPO_4$, pH 7.2) at 37°C for 2-4 hours and 48-72 hours, respectively. After destained with absolute ethanol at room temperature for 2 hours, the samples were immersed in Lugol's solution (Sigma Aldrich) for 10 s, and fixed and mounted with clearing solution [chloral

hydrate:water:glycerol = 8:3:1, w/v/v). Images were captured by a differential interference contrast (DIC) microscopy (Leica DMC4500), with HC PL FLUOTAR 40×/0.80 objective.

EdU staining

EdU staining was performed following the modified protocol of the YF® 555 Click-iT EdU imaging kit (US EVERBRIGHT), as described below. Seedlings (4.0-4.5 DAG) grown on ½ MS medium were transferred to the ½ MS medium with 2.5 μM EdU for 12 hours, then excised root tips and immersed into 3.7% formaldehyde in PBS buffer (pH=7.3) for fixing 30 minutes at 4°C, then washed the samples with PBS buffer (pH=7.3). Added 0.5% Triton X-100 in PBS buffer (pH=7.3), incubated at room temperature for 20 minutes. After washing with PBS buffer (pH=7.3), samples were immersed in Click-iT working solution [1× Click-iT EdU reaction buffer (860 μL/mL), $CuSO_4$ (40 μL/mL), YF® 555 Azide (2 μL/mL), 1× Click-iT EdU buffer additives (100 μL/mL)] for 30 minutes in darkness. Then washed the samples with PBS buffer (pH=7.3), and transferred onto slides and covered with a drop of water, a coverslip was placed on top before observation. Images were captured by the Leica TCS SP8 multiphoton (MP) system with the HC PL APO 20×/0.75 CS2 objective, EdU fluorescence signals were detected by exciting with laser at 552 nm, and by collecting emission from 600-650 nm on a PMT detector and a TLD detector (552 nm PMT trans). All images were acquired by using the Leica Application Suite X software 3.5.2.18963.

QUANTIFICATION AND STATISTICAL ANALYSIS

Quantification of GFP intensity in QC area and SI/SID area were analyzed using software of Leica LAS AF lite (quantify, sort in ROIs, mean value). All values were analyzed using GraphPad Prism (version 8.3.0) and Excel, significance of difference was examined by Student's t test, results were considered significant when $p < 0.05$. All data were presented with mean ± SD. Statistical tests, p values, number of biological and technical replicates, and number of independent experiments are indicated in the figure and figure legends.

References

Aida, M., Beis, D., Heidstra, R., Willemsen, V., Blilou, I., Galinha, C., Nussaume, L., Noh, Y.-S., Amasino, R., and Scheres, B. (2004). The PLETHORA genes mediate patterning of the Arabidopsis root stem cell niche. Cell *119*, 109-120.

Ali, A., Hoeflich, K.P., and Woodgett, J.R. (2001). Glycogen synthase kinase-3: properties, functions, and regulation. Chemical reviews *101*, 2527-2540.

Ardito, F., Giuliani, M., Perrone, D., Troiano, G., and Lo Muzio, L. (2017). The crucial role of protein phosphorylation in cell signaling and its use as targeted therapy (Review). Int J Mol Med *40*, 271-280.

Ballesteros, I., Dominguez, T., Sauer, M., Paredes, P., Duprat, A., Rojo, E., Sanmartin, M., and Sanchez-Serrano, J.J. (2013). Specialized functions of the PP2A subfamily II catalytic subunits PP2A-C3 and PP2A-C4 in the distribution of auxin fluxes and development in Arabidopsis. The Plant journal : for cell and molecular biology *73*, 862-872.

1082 Barlow, P.W. (2015a). The concept of the quiescent centre and how it found support from work
1083 with X-rays. I. Historical perspectives. Plant Root *9*, 43-55.
1084 Barlow, P.W. (2015b). The concept of the quiescent centre and how it found support from work
1085 with X-rays. II. The molecular aftermath. Plant Root *9*, 56-67.
1086 Barlow, P.W. (2015c). Origin of the concept of the quiescent centre of plant roots. Protoplasma
1087 *253*, 1-15.
1088 Belizario, J.E., Alves, J., Garay-Malpartida, M., and Occhiucci, J.M. (2008). Coupling caspase
1089 cleavage and proteasomal degradation of proteins carrying PEST motif. Current protein &
1090 peptide science *9*, 210-220.
1091 Berckmans, B., Kirschner, G., Gerlitz, N., Stadler, R., and Simon, R. (2020). CLE40 signalling
1092 regulates the fate of root stem cells in Arabidopsis. Plant Physiology, pp.00914.02019.
1093 Bian, C., Guo, X., Zhang, Y., Wang, L., Xu, T., DeLong, A., and Dong, J. (2020). Protein
1094 phosphatase 2A promotes stomatal development by stabilizing SPEECHLESS in Arabidopsis. Proc
1095 Natl Acad Sci U S A *117*, 13127-13137.
1096 Brand, A.H., and Perrimon, N. (1993). Targeted gene expression as a means of altering cell fates
1097 and generating dominant phenotypes. Development *118*, 401-415.
1098 Bu, S.L., Liu, C., Liu, N., Zhao, J.L., Ai, L.F., Chi, H., Li, K.L., Chien, C.W., Burlingame, A.L., Zhang,
1099 S.W.*, et al.* (2017). Immunopurification and Mass Spectrometry Identifies Protein Phosphatase
1100 2A (PP2A) and BIN2/GSK3 as Regulators of AKS Transcription Factors in Arabidopsis. Mol Plant
1101 *10*, 345-348.
1102 Burkart, R.C., Strotmann, V.I., Kirschner, G.K., Akinci, A., Czempik, L., Maizel, A., Weidtkamp-
1103 Peters, S., and Stahl, Y. (2019). PLETHORA and WOX5 interaction and subnuclear localisation
1104 regulates Arabidopsis root stem cell maintenance. bioRxiv, 818187.
1105 Celine, F., Ernst, A., Emily, S., Viola, W., Thomas, L., Walter, D., and Murray, J.A.H. (2014). WOX5
1106 suppresses CYCLIN D activity to establish quiescence at the center of the root stem cell niche.
1107 Current Biology *24*, 1939-1944.
1108 Chen, K., Li, G.J., Bressan, R.A., Song, C.P., Zhu, J.K., and Zhao, Y. (2020). Abscisic acid dynamics,
1109 signaling, and functions in plants. J Integr Plant Biol *62*, 25-54.
1110 Clark, N.M., Fisher, A.P., Berckmans, B., Van den Broeck, L., Nelson, E.C., Nguyen, T.T., Bustillo-
1111 Avendano, E., Zebell, S.G., Moreno-Risueno, M.A., Simon, R.*, et al.* (2020). Protein complex
1112 stoichiometry and expression dynamics of transcription factors modulate stem cell division. Proc
1113 Natl Acad Sci U S A *117*, 15332-15342.
1114 Claudia, V.D.B., Willemsen, V., Hendriks, G., Weisbeek, P., and Scheres, B. (1997). Short-range
1115 control of cell differentiation in the Arabidopsis root meristem. *390*, 287-289.
1116 Clevers, H., Loh, K.M., and Nusse, R. (2014). An integral program for tissue renewal and
1117 regeneration: Wnt signaling and stem cell control. Science *346*, 1248012.
1118 Clowes, F.A.L. (1961). Effects of β-radiation on meristems. Experimental Cell Research *25*, 529-
1119 534.
1120 Clowes, F.A.L. (1963). X-Irradiation of Root Meristems. Annals of Botany *27*, 343-352.
1121 Clowes, F.A.L. (1968). THE DNA CONTENT OF THE CELLS OF THE QUIESCENT CENTRE AND ROOT
1122 CAP OF ZEA MAYS. New Phytol *67*, 631-639.
1123 Clowes, F.A.L. (1981). The Difference between Open and Closed Meristems. Annals of Botany *48*,
1124 761-767.
1125 Cruz-Ramírez, A., Díaz-Triviño, S., Blilou, I., Grieneisen, V.A., Sozzani, R., Zamioudis, C., Miskolczi,
1126 P., Nieuwland, J., Benjamins, R., and Dhonukshe, P. (2012). A bistable circuit involving
1127 SCARECROW-RETINOBLASTOMA integrates cues to inform asymmetric stem cell division. Cell
1128 *150*, 1002-1015.

1129 Cruz-Ramírez, A., Díaz-Triviño, S., Wachsman, G., Du, Y., Arteága-Vázquez, M., Zhang, H.,
1130 Benjamins, R., Blilou, I., Neef, A.B., and Chandler, V. (2013). A SCARECROW-RETINOBLASTOMA
1131 protein network controls protective quiescence in the Arabidopsis root stem cell organizer. PLoS
1132 biology *11*.
1133 De Rybel, B., Audenaert, D., Vert, G., Rozhon, W., Mayerhofer, J., Peelman, F., Coutuer, S.,
1134 Denayer, T., Jansen, L., Nguyen, L.*, et al.* (2009). Chemical Inhibition of a Subset of Arabidopsis
1135 thaliana GSK3-like Kinases Activates Brassinosteroid Signaling. Chemistry & Biology *16*, 594-604.
1136 Di Rubbo, S., Irani, N.G., and Russinova, E. (2011). PP2A Phosphatases: The "On-Off" Regulatory
1137 Switches of Brassinosteroid Signaling. Science Signaling *4*, pe25-pe25.
1138 Dolan, L., Janmaat, K., Willemsen, V., Linstead, P., Poethig, S., Roberts, K., and Scheres, B. (1993).
1139 Cellular organisation of the Arabidopsis thaliana root. Development *119*, 71-84.
1140 Dolzblasz, A., Nardmann, J., Clerici, E., Causier, B., van der Graaff, E., Chen, J., Davies, B., Werr,
1141 W., and Laux, T. (2016). Stem Cell Regulation by Arabidopsis WOX Genes. Mol Plant *9*, 1028-
1142 1039.
1143 Dubrovsky, J.G., and Barlow, P.W. (2015). The origins of the quiescent centre concept. New
1144 Phytol *206*.
1145 Fiol, C.J., Wang, A., Roeske, R.W., and Roach, P.J. (1990). Ordered multisite protein
1146 phosphorylation. Analysis of glycogen synthase kinase 3 action using model peptide substrates.
1147 The Journal of biological chemistry *265*, 6061-6065.
1148 Haecker, A., Groß-Hardt, R., Geiges, B., Sarkar, A., Breuninger, H., Herrmann, M., and Laux, T.
1149 (2004). Expression dynamics of WOXgenes mark cell fate decisions during early embryonic
1150 patterning in Arabidopsis thaliana. Development *131*, 657-668.
1151 He, G., Liu, J., Dong, H., and Sun, J. (2019). The Blue-Light Receptor CRY1 Interacts with BZR1 and
1152 BIN2 to Modulate the Phosphorylation and Nuclear Function of BZR1 in Repressing BR Signaling
1153 in Arabidopsis. Mol Plant *12*, 689-703.
1154 He, J.-X., Gendron, J.M., Yang, Y., Li, J., and Wang, Z.-Y. (2002). The GSK3-like kinase BIN2
1155 phosphorylates and destabilizes BZR1, a positive regulator of the brassinosteroid signaling
1156 pathway in Arabidopsis. Proceedings of the National Academy of Sciences *99*,
1157 10185-10190.
1158 Houbaert, A., Zhang, C., Tiwari, M., Wang, K., de Marcos Serrano, A., Savatin, D.V., Urs, M.J.,
1159 Zhiponova, M.K., Gudesblat, G.E., Vanhoutte, I.*, et al.* (2018). POLAR-guided signalling complex
1160 assembly and localization drive asymmetric cell division. Nature *563*, 574-578.
1161 Hu, Y., and Yu, D. (2014). BRASSINOSTEROID INSENSITIVE2 interacts with ABSCISIC ACID
1162 INSENSITIVE5 to mediate the antagonism of brassinosteroids to abscisic acid during seed
1163 germination in Arabidopsis. Plant Cell *26*, 4394-4408.
1164 Jefri, H., Toon, C., Filip, V., Heyndrickx, K.S., Jelle, V.L., Ilse, V., Sandy, V., Klaas, V., Geert, D.J.,
1165 and Dominique, V.D.S. (2013). ERF115 controls root quiescent center cell division and stem cell
1166 replenishment. Science *342*, 860-863.
1167 Kotogány, E., Dudits, D., Horváth, G.V., and Ayaydin, F. (2010). A rapid and robust assay for
1168 detection of S-phase cell cycle progression in plant cells and tissues by using ethynyl
1169 deoxyuridine. Plant methods *6*, 5-5.
1170 Kumpf, R., Thorstensen, T., Rahman, M.A., Heyman, J., Nenseth, H.Z., Lammens, T., Herrmann,
1171 U., Swarup, R., Veiseth, S.V., Emberland, G.*, et al.* (2014). The ASH1-RELATED3 SET-domain
1172 protein controls cell division competence of the meristem and the quiescent center of the
1173 Arabidopsis primary root. Plant Physiol *166*, 632-643.
1174 Laurenzio, L.D., Wysocka-Diller, J., Malamy, J.E., Pysh, L., Helariutta, Y., Freshour, G., Hahn, M.G.,
1175 Feldmann, K.A., and Benfey, P.N. (1996). The SCARECROW Gene Regulates an Asymmetric Cell

1176 Division That Is Essential for Generating the Radial Organization of the Arabidopsis Root. Cell *86*,
1177 0-433.
1178 Li, J., Zhou, H., Zhang, Y., Li, Z., Yang, Y., and Guo, Y. (2020). The GSK3-like Kinase BIN2 Is a
1179 Molecular Switch between the Salt Stress Response and Growth Recovery in Arabidopsis
1180 thaliana. Dev Cell *55*, 367-380 e366.
1181 Li, L., and Clevers, H. (2010). Coexistence of quiescent and active adult stem cells in mammals.
1182 Science *327*, 542-545.
1183 Li, Y.M., and Casida, J.E. (1992). Cantharidin-binding protein: identification as protein
1184 phosphatase 2A. Proc Natl Acad Sci U S A *89*, 11867-11870.
1185 Long, Y., Smet, W., Cruz-Ramírez, A., Castelijns, B., de Jonge, W., Mähönen, A.P., Bouchet, B.P.,
1186 Perez, G.S., Akhmanova, A., Scheres, B.*, et al.* (2015). Arabidopsis BIRD Zinc Finger Proteins
1187 Jointly Stabilize Tissue Boundaries by Confining the Cell Fate Regulator SHORT-ROOT and
1188 Contributing to Fate Specification. The Plant Cell *27*, 1185-1199.
1189 Long, Y., Stahl, Y., Weidtkamp-Peters, S., Postma, M., Zhou, W., Goedhart, J., Sánchez-Pérez, M.-
1190 I., Gadella, T.W.J., Simon, R., Scheres, B.*, et al.* (2017). In vivo FRET–FLIM reveals cell-type-
1191 specific protein interactions in Arabidopsis roots. Nature *548*, 97-102.
1192 Lu, R., Canher, B., Bisht, A., Heyman, J., and De Veylder, L. (2021). Three-dimensional
1193 quantitative analysis of the Arabidopsis quiescent center. Journal of Experimental Botany.
1194 MacDonald, B.T., Tamai, K., and He, X. (2009). Wnt/β-Catenin Signaling: Components,
1195 Mechanisms, and Diseases. Developmental Cell *17*, 9-26.
1196 Matosevich, R., and Efroni, I. (2021). The quiescent center and root regeneration. J Exp Bot *72*,
1197 6739-6745.
1198 Meyer, R.D., Srinivasan, S., Singh, A.J., Mahoney, J.E., Gharahassanlou, K.R., and Rahimi, N.
1199 (2011). PEST motif serine and tyrosine phosphorylation controls vascular endothelial growth
1200 factor receptor 2 stability and downregulation. Mol Cell Biol *31*, 2010-2025.
1201 Nakajima, K., ., Sena, G., ., Nawy, T., ., and Benfey, P.N. (2001). Intercellular movement of the
1202 putative transcription factor SHR in root patterning. Nature *413*, 307-311.
1203 Patel, P., and Woodgett, J.R. (2017). Glycogen Synthase Kinase 3: A Kinase for All Pathways? Curr
1204 Top Dev Biol *123*, 277-302.
1205 Pi, L., Aichinger, E., Vandergraaff, E., Llavata-Peris, C., Weijers, D., Hennig, L., Groot, E., and Laux,
1206 T. (2015). Organizer-Derived WOX5 Signal Maintains Root Columella Stem Cells through
1207 Chromatin-Mediated Repression of CDF4 Expression. Developmental Cell *33*, 576-588.
1208 Planas-Riverola, A., Gupta, A., Betegon-Putze, I., Bosch, N., Ibanes, M., and Cano-Delgado, A.I.
1209 (2019). Brassinosteroid signaling in plant development and adaptation to stress. Development
1210 *146*.
1211 Rahman, A., Takahashi, M., Shibasaki, K., Wu, S., Inaba, T., Tsurumi, S., and Baskin, T.I. (2010).
1212 Gravitropism of Arabidopsis thaliana roots requires the polarization of PIN2 toward the root tip
1213 in meristematic cortical cells. The Plant cell *22*, 1762-1776.
1214 Rahni, R., and Birnbaum, K.D. (2019). Week-long imaging of cell divisions in the Arabidopsis root
1215 meristem. Plant Methods *15*.
1216 Rechsteiner, M., and Rogers, S.W. (1996). PEST sequences and regulation by proteolysis. Trends
1217 in biochemical sciences *21*, 267-271.
1218 Rodriguez, K., Perales, M., Snipes, S., Yadav, R.K., Diaz-Mendoza, M., and Reddy, G.V. (2016).
1219 DNA-dependent homodimerization, sub-cellular partitioning, and protein destabilization control
1220 WUSCHEL levels and spatial patterning. Proc Natl Acad Sci U S A *113*, E6307-E6315.
1221 Rogers, S., Wells, R., and Rechsteiner, M. (1986). Amino acid sequences common to rapidly
1222 degraded proteins: the PEST hypothesis. Science *234*, 364-368.

1223 Sabatini, S., Heidstra, R., Wildwater, M., and Scheres, B. (2003). SCARECROW is involved in
1224 positioning the stem cell niche in the Arabidopsis root meristem. Genes Dev *17*, 354-358.
1225 Sandhu, K.S., and Dash, D. (2006). Conformational flexibility may explain multiple cellular roles
1226 of PEST motifs. Proteins: Structure, Function, and Bioinformatics *63*, 727-732.
1227 Sarkar, A.K., Luijten, M., Miyashima, S., Lenhard, M., Hashimoto, T., Nakajima, K., Scheres, B.,
1228 Heidstra, R., and Laux, T. (2007). Conserved factors regulate signalling in Arabidopsis thaliana
1229 shoot and root stem cell organizers. Nature *446*, 811-814.
1230 Savina, M.S., Pasternak, T., Omelyanchuk, N.A., Novikova, D.D., Palme, K., Mironova, V.V., and
1231 Lavrekha, V.V. (2020). Cell Dynamics in WOX5-Overexpressing Root Tips: The Impact of Local
1232 Auxin Biosynthesis. Front Plant Sci *11*, 560169.
1233 Shi, Y. (2009). Serine/threonine phosphatases: mechanism through structure. Cell *139*, 468-484.
1234 Shimotohno, A., Heidstra, R., Blilou, I., and Scheres, B. (2018). Root stem cell niche organizer
1235 specification by molecular convergence of PLETHORA and SCARECROW transcription factor
1236 modules. Genes & development *32*, 1085-1100.
1237 Sokol, S.Y. (2011). Maintaining embryonic stem cell pluripotency with Wnt signaling.
1238 Development *138*, 4341-4350.
1239 Spinner, L., Gadeyne, A., Belcram, K., Goussot, M., Moison, M., Duroc, Y., Eeckhout, D., De
1240 Winne, N., Schaefer, E., Van De Slijke, E.*, et al.* (2013). A protein phosphatase 2A complex
1241 spatially controls plant cell division. Nat Commun *4*, 1863.
1242 Stahl, Y., Grabowski, S., Bleckmann, A., Kühnemuth, R., Weidtkamp-Peters, S., Pinto, Karine G.,
1243 Kirschner, Gwendolyn K., Schmid, Julia B., Wink, René H., Hülsewede, A.*, et al.* (2013).
1244 Moderation of Arabidopsis Root Stemness by CLAVATA1 and ARABIDOPSIS CRINKLY4 Receptor
1245 Kinase Complexes. Current Biology *23*, 362-371.
1246 Stahl, Y., Wink, R.H., Ingram, G.C., and Simon, R. (2009). A Signaling Module Controlling the Stem
1247 Cell Niche in Arabidopsis Root Meristems. Current Biology *19*, 909-914.
1248 Su, Y., Fu, C., Ishikawa, S., Stella, A., Kojima, M., Shitoh, K., Schreiber, E.M., Day, B.W., and Liu, B.
1249 (2008). APC Is Essential for Targeting Phosphorylated β-Catenin to the SCFβ-TrCP Ubiquitin
1250 Ligase. Molecular Cell *32*, 652-661.
1251 Tan, S., Luschnig, C., and Friml, J. (2021). Pho-view of Auxin: Reversible Protein Phosphorylation
1252 in Auxin Biosynthesis, Transport and Signaling. Mol Plant *14*, 151-165.
1253 Tang, W., Yuan, M., Wang, R., Yang, Y., Wang, C., Oses-Prieto, J.A., Kim, T.W., Zhou, H.W., Deng,
1254 Z., Gampala, S.S.*, et al.* (2011). PP2A activates brassinosteroid-responsive gene expression and
1255 plant growth by dephosphorylating BZR1. Nat Cell Biol *13*, 124-131.
1256 Tian, H., Wabnik, K., Niu, T., Li, H., Yu, Q., Pollmann, S., Vanneste, S., Govaerts, W., Rolcik, J.,
1257 Geisler, M.*, et al.* (2014). WOX5-IAA17 feedback circuit-mediated cellular auxin response is
1258 crucial for the patterning of root stem cell niches in Arabidopsis. Mol Plant *7*, 277-289.
1259 Truernit, E., Bauby, H., Dubreucq, B., Grandjean, O., Runions, J., Barthelemy, J., and Palauqui, J.C.
1260 (2008). High-resolution whole-mount imaging of three-dimensional tissue organization and gene
1261 expression enables the study of Phloem development and structure in Arabidopsis. Plant Cell *20*,
1262 1494-1503.
1263 Ubogoeva, E.V., Zemlyanskaya, E.V., Xu, J., and Mironova, V. (2021). Mechanisms of stress
1264 response in the root stem cell niche. J Exp Bot *72*, 6746-6754.
1265 Vanstraelen, M., Baloban, M., Da Ines, O., Cultrone, A., Lammens, T., Boudolf, V., Brown, S.C., De
1266 Veylder, L., Mergaert, P., and Kondorosi, E. (2009). APC/C^{CCS52A} complexes control meristem
1267 maintenance in the Arabidopsis root. Proceedings of the National Academy of
1268 Sciences *106*, 11806-11811.

1269 Vilarrasablasi, J., Gonzálezgarcía, M.P., Frigola, D., Fàbregas, N., Alexiou, K.G., Lópezbigas, N.,
1270 Rivas, S., Jauneau, A., Lohmann, J.U., and Benfey, P.N. (2014). Regulation of plant stem cell
1271 quiescence by a brassinosteroid signaling module. Developmental Cell *30*, 36-47.
1272 Walter, M., Chaban, C., Schutze, K., Batistic, O., Weckermann, K., Nake, C., Blazevic, D., Grefen,
1273 C., Schumacher, K., Oecking, C.*, et al.* (2004). Visualization of protein interactions in living plant
1274 cells using bimolecular fluorescence complementation. The Plant journal : for cell and molecular
1275 biology *40*, 428-438.
1276 Worby, C.A., and Dixon, J.E. (2019). Reversible phosphorylation: a birthday tribute to Herb Tabor.
1277 The Journal of biological chemistry *294*, 1638-1642.
1278 Yadav, R.K., Perales, M., Gruel, J., Girke, T., Jönsson, H., and Reddy, G.V. (2011). WUSCHEL
1279 protein movement mediates stem cell homeostasis in the Arabidopsis shoot apex. Genes &
1280 development *25*, 2025-2030.
1281 Yamamoto, H., Kishida, S., Kishida, M., Ikeda, S., Takada, S., and Kikuchi, A. (1999).
1282 Phosphorylation of Axin, a Wnt Signal Negative Regulator, by Glycogen Synthase Kinase-3β
1283 Regulates Its Stability*. Journal of Biological Chemistry *274*, 10681-10684.
1284 Yan, Z., Zhao, J., Peng, P., Chihara, R.K., and Li, J. (2009). BIN2 functions redundantly with other
1285 Arabidopsis GSK3-like kinases to regulate brassinosteroid signaling. Plant Physiol *150*, 710-721.
1286 Ye, H., Li, L., Guo, H., and Yin, Y. (2012). MYBL2 is a substrate of GSK3-like kinase BIN2 and acts
1287 as a corepressor of BES1 in brassinosteroid signaling pathway in Arabidopsis. Proc Natl Acad Sci
1288 U S A *109*, 20142-20147.
1289 Youn, J.H., and Kim, T.W. (2015). Functional insights of plant GSK3-like kinases: multi-taskers in
1290 diverse cellular signal transduction pathways. Mol Plant *8*, 552-565.
1291 Zhai, H., Zhang, X., You, Y., Lin, L., Zhou, W., and Li, C. (2020). SEUSS integrates transcriptional
1292 and epigenetic control of root stem cell organizer specification. Embo j, e105047.
1293 Zhang, Y., Jiao, Y., Liu, Z., and Zhu, Y.X. (2015). ROW1 maintains quiescent centre identity by
1294 confining WOX5 expression to specific cells. Nature Communications *6*, 6003.
1295 Zhou, Y., Yan, A., Han, H., Li, T., Geng, Y., Liu, X., and Meyerowitz, E.M. (2018). HAIRY MERISTEM
1296 with WUSCHEL confines CLAVATA3 expression to the outer apical meristem layers. Science *361*,
1297 502-506.
1298 Zhu, Y., Hu, C., Cui, Y., Zeng, L., Li, S., Zhu, M., Meng, F., Huang, S., Long, L., Yi, J.*, et al.* (2021).
1299 Conserved and differentiated functions of CIK receptor kinases in modulating stem cell signaling
1300 in Arabidopsis. Mol Plant *14*, 1119-1134.

1301

All Main Figures

Ling Chen

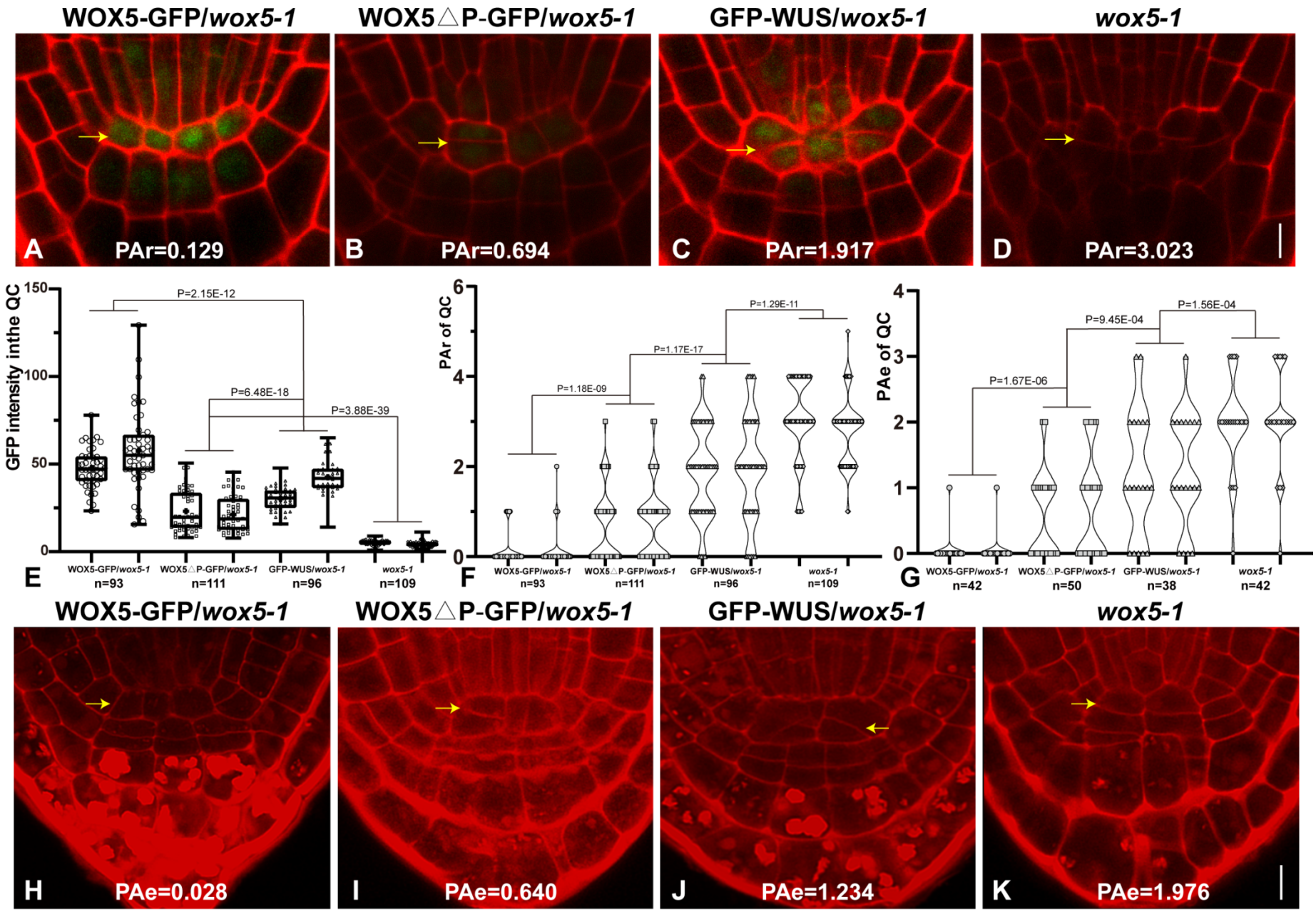

Figure 1: The PEST domain stabilizes WOX5 protein and maintains low proliferative activity of QC cells from the embryonic stage to the post-embryonic stage.

Figure 1: The PEST domain stabilizes WOX5 protein and maintains low proliferative activity of QC cells from the embryonic stage to the post-embryonic stage.

(A~D) PI staining images of (A) WOX5-GFP/*wox5-1* rescued lines (PAr = 0.129); (B) WOX5△PEST-GFP/*wox5-1* rescued lines (PAr = 0.694); (C) GFP-WUS/*wox5-1* rescued lines (PAr = 1.917); (D) *wox5-1* (PAr = 3.023).

(E) GFP intensity in the QC at 5DAG of 93 strains of WOX5-GFP/*wox5-1* rescued lines (46 strains of W5-3 line plus 47 strains of W5-4 line); of 111 strains of WOX5△PEST-GFP/*wox5-1* rescued lines (55 strains of dP-2 line plus 56 strains of dP-3 line); of 96 strains of GFP-WUS/*wox5-1* rescued lines (49 strains of WU-1 line plus 47 strains of WU-2 line); and of 109 strains of *wox5-1*.

(F) PAr of QC at 5DAG of 93 strains of WOX5-GFP/*wox5-1* rescued lines (46 strains of W5-3 line plus 47 strains of W5-4 line); of 111 strains of WOX5△PEST-GFP/*wox5-1* rescued lines (55 strains of dP-2 line plus 56 strains of dP-3 line); of 96 strains of GFP-WUS/*wox5-1* rescued lines (49 strains of WU-1 line plus 47 strains of WU-2 line); and of 109 strains of *wox5-1*.

(G) PAe of QC at the mature embryonic stage of 42 strains of WOX5-GFP/*wox5-1* rescued lines (21 strains of W5-3 line plus 21 strains of W5-4 line); of 50 strains of WOX5△PEST-GFP/*wox5-1* rescued lines (25 strains of dP-2 line plus 25 strains of dP-3 line); of 38 strains of GFP-WUS/*wox5-1* rescued lines (19 strains of WU-1 line plus 19 strains of WU-2 line); and of 42 strains of *wox5-1*.

(H~K) mPS-PI staining images of (H) WOX5-GFP/*wox5-1* rescued lines (PAe = 0.028); (I) WOX5△PEST-GFP/*wox5-1* rescued lines (PAe = 0.640); (J) GFP-WUS/*wox5-1* rescued lines (PAe = 1.234); (K) *wox5-1* (PAe = 1.976).

Student t test indicates statistical difference. Bar = 10 μm, yellow arrows show the QC cells or the cell plates of QC cells.

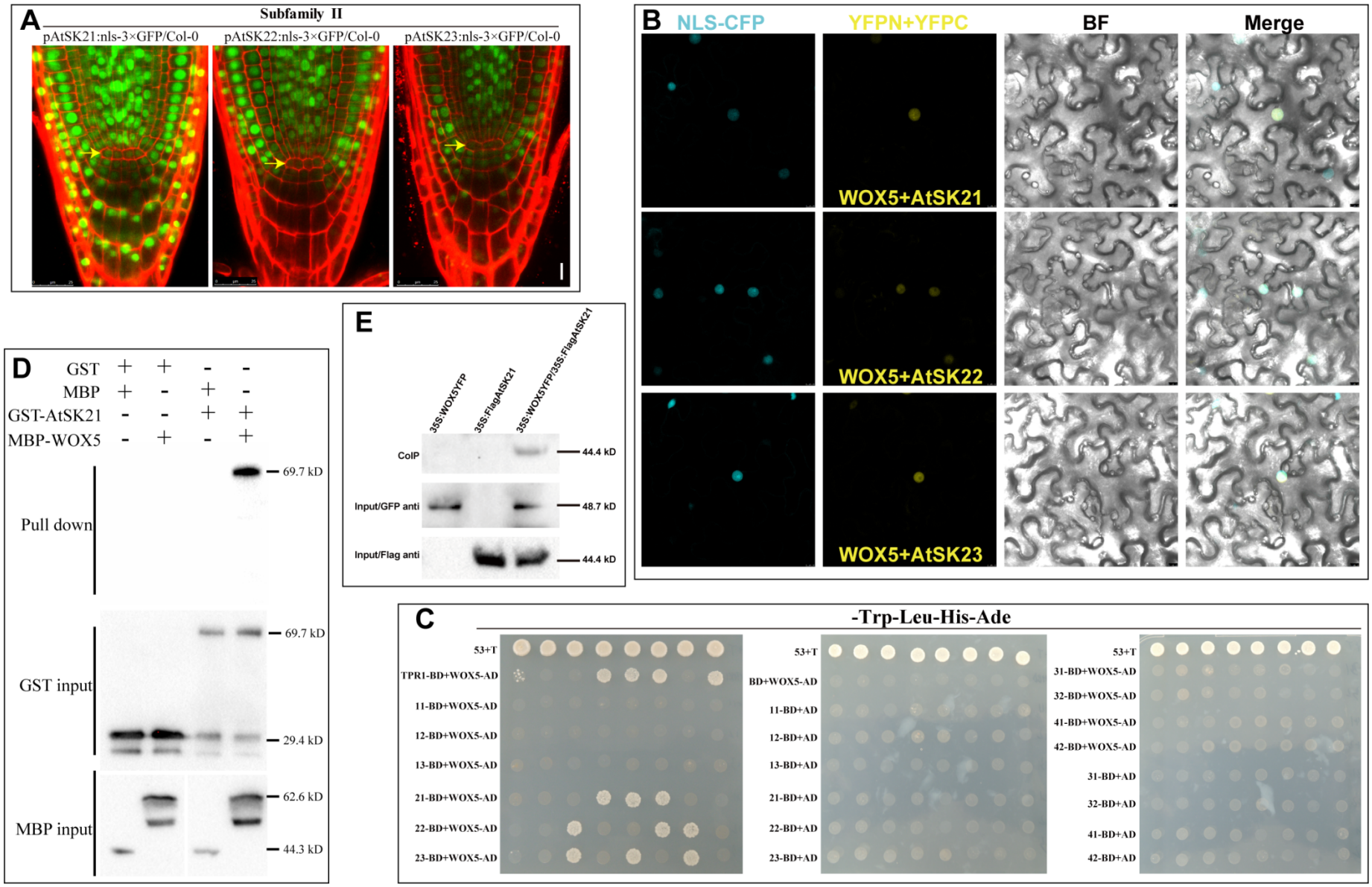

Figure 2: **The subfamily II of AtSKs (AtSK21, AtSK22, AtSK23) interact with WOX5 in vitro and in vivo.**

Figure 2: The subfamily II of AtSKs (AtSK21, AtSK22, AtSK23) interact with WOX5 in vitro and in vivo.

(A) Transcriptional reporters of the subfamily II of AtSKs (AtSK21, AtSK22 and AtSK23) all expressed in the QC at 5DAG.
(B) BiFC assay: NLS-CFP is a nuclear marker, YFPN+YFPC means WOX5-YFPN interacted with AtSK21-YFPC, AtSK22-YFPC and AtSK23-YFPC in nucleus in *the nicotiana tabacum*, , BF is bright filed.
(C) Y2H assay: In the Yeast Base Medium without Trp, Leu, His and Ade, the AH109 strain of positive control groups 53+T all grew (8/8), and TPR1-BD+WOX5-AD mostly grew (5/8); only experiment groups AtSK21-BD+WOX5-AD, AtSK22-BD+WOX5-AD and AtSK23-BD+WOX5-AD grew some (3/8), but experiment groups AtSK11-BD+WOX5-AD, AtSK12-BD+WOX5-AD, AtSK13-BD+WOX5-AD, AtSK31-BD+WOX5-AD, AtSK32-BD+WOX5-AD, AtSK41-BD+WOX5-AD, AtSK42-BD+WOX5-AD not grew (0/8); the negative control groups AtSK11-BD+AD, AtSK12-BD+AD, AtSK13-BD+AD, AtSK21-BD+AD, AtSK22-BD+AD and AtSK23-BD+AD, AtSK31-BD+AD, AtSK32-BD+AD, AtSK41-BD+AD, AtSK42-BD+AD all not grew (0/8).
(D) Pull down in vitro assay: MBP input means MBP protein (44.3 kD) and MBP-WOX5 protein (62.6 kD) exist in the transfer membrane presenting by MBP mouse anti; GST input means GST protein (29.4 kD) and GST-AtSK21 (69.7 kD) exist in the transfer membrane presenting by GST mouse anti; Pull down means only when MBP-WOX5 protein and GST-AtSK21 protein both exist in reaction solution, the GST-AtSK21 protein (69.7 kD) could be pull down by MBP beads.
(E) CoIP assay: 35S:WOX5YFP is 35S : LhGR-pOp : WOX5-YFP/Col-0 line, 35S:FlagAtSK21 is 35S : Flag-AtSK21/Col-0 line, 35S:WOX5YFP/ 35S:FlagAtSK21 means the double homozygous line of 35S : LhGR-pOp : WOX5-YFP/Col-0 line cross to 35S : Flag-AtSK21/Col-0 line. Input/GFP anti means WOX5YFP protein (48.7 kD) exist in the transfer membrane presenting by GFP mouse anti, Input/Flag anti means FlagAtSK21 protein (44.4 kD) exist in the transfer membrane presenting by Flag mouse anti, CoIP means Flag-AtSK21 protein could be co-immunoprecipitated by GFP beads only in the double homozygous line.
Bar = 10 μm, yellow arrows show the QC cells.

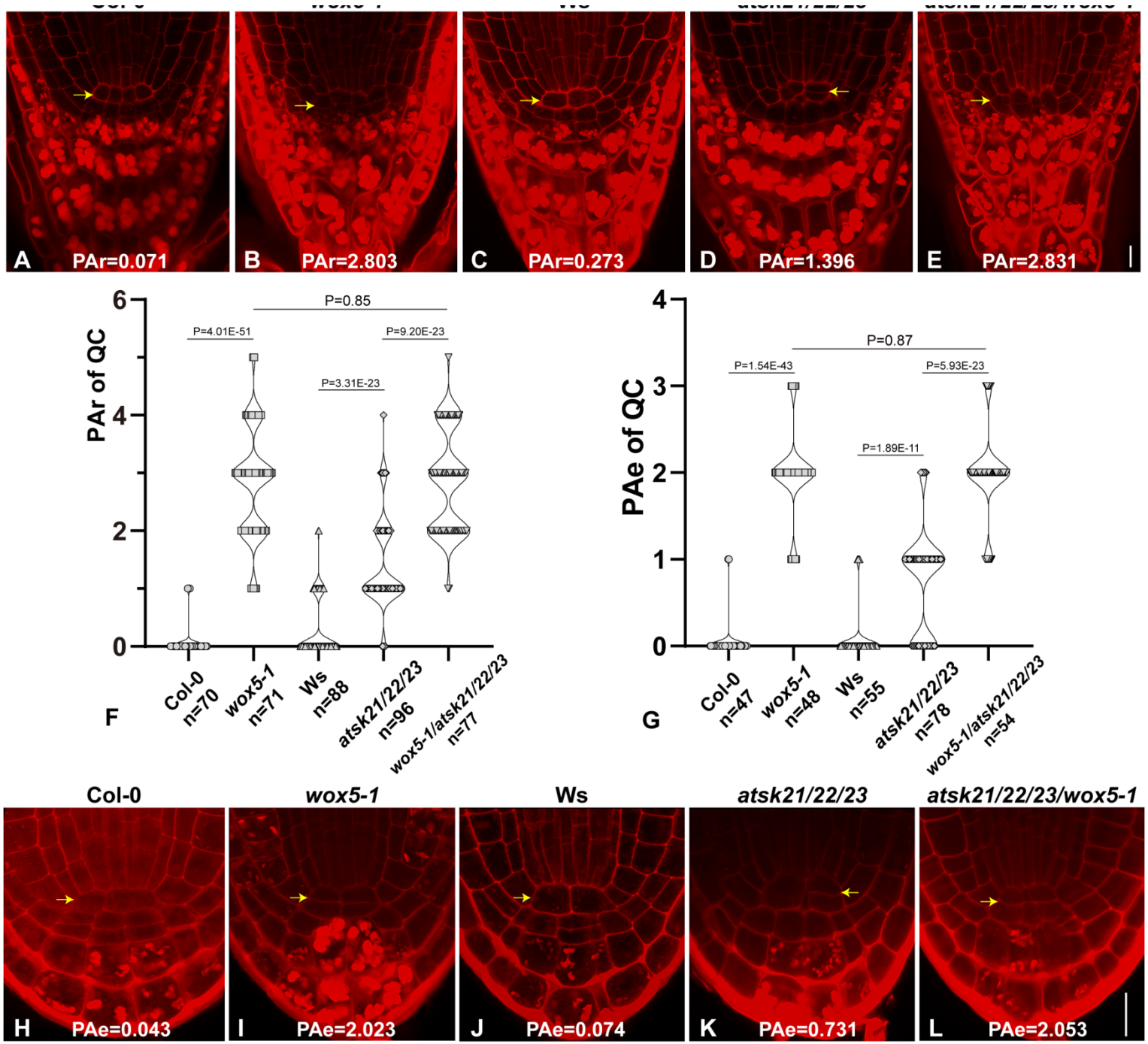

Figure 3: **WOX5 is epistatic to the subfamily II of AtSKs in inhibiting proliferative activity of QC**

Figure 3: WOX5 is epistatic to the subfamily II of AtSKs in inhibiting proliferative activity of QC cells from the embryonic stage to the post-embryonic stage.

(A~E) mPS-PI staining images of (A) Col-0 (PAr = 0.071); (B) *wox5-1* (PAr = 2.803; (C) *Wassilewskija* (Ws) (PAr = 0.273); (D) *atsk21/22/23* (PAr = 1.396); (E) *atsk21/22/23wox5-1* (PAr = 2.831).
(F) PAr of QC at 5DAG of Col-0 (n=70), *wox5-1* (n=71), Ws (n=88), *atsk21/22/23* (n=96), *atsk21/22/23wox5-1* (n=77).
(G) PAe of QC at the mature embryonic stage of Col-0 (n=46), *wox5-1* (n=48), Ws (n=55), *atsk21/22/23* (n=78), *atsk21/22/23wox5-1* (n=54).
(H~L) mPS-PI staining images of (H) Col-0 (PAe = 0.059); (I) *wox5-1* (PAe = 2.023; (J) Ws (PAe = 0.073); (K) *atsk21/22/23* (PAe = 0.731); (L) *atsk21/22/23wox5-1* (PAe = 2.053).
Student t test indicates statistical difference, bar = 10 μm, yellow arrows show the QC cells or the cell plates of QC cells.

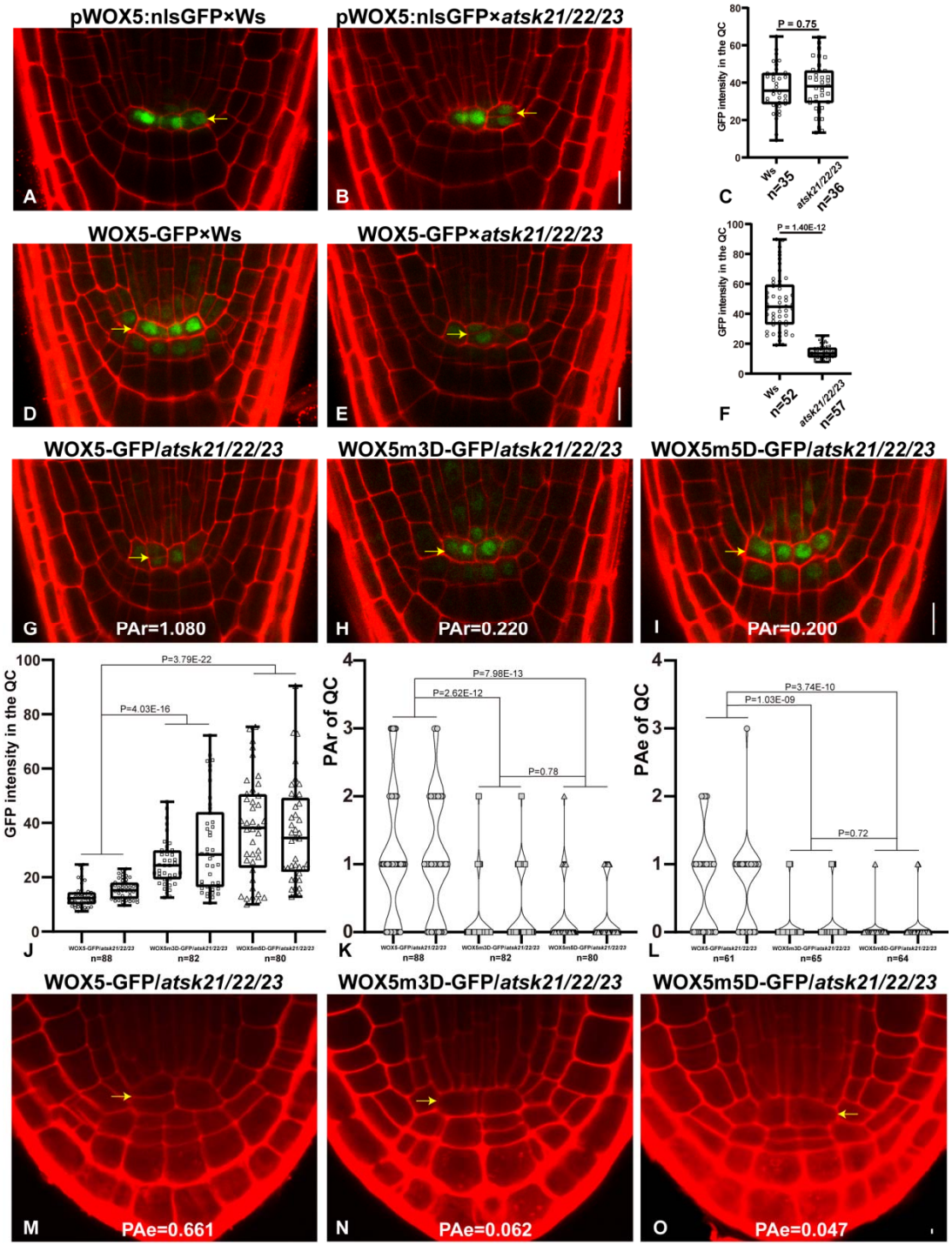

Figure 4: The subfamily II of AtSKs stabilize WOX5 protein by phosphorylating the GMs.

Figure 4: The subfamily II of AtSKs stabilize WOX5 protein by phosphorylating the GMs.

(A,B) PI staining images of (A) pWOX5:nlsGFP×Ws and (B) pWOX5:nlsGFP×*atsk21/22/23*;
(C) GFP intensity in the QC at 5DAG of pWOX5:nlsGFP×Ws (n=35) and pWOX5:nlsGFP×*atsk21/22/23* (n=36).
(D,E) PI staining images of (D) pWOX5:WOX5GFP×Ws and (E) pWOX5:WOX5GFP×*atsk21/22/23*;
(F) GFP intensity in the QC at 5DAG of pWOX5:WOX5GFP×Ws (n=52) and pWOX5:WOX5GFP×*atsk21/22/23* (n=57).
(G~I) PI staining images of WOX5GFP/*atsk21/22/23* line (PAr = 1.080), WOX5m3DGFP/*atsk21/22/23* line (PAr = 0.220) and WOX5m5DGFP/*atsk21/22/23* line (PAr = 0.200).
(J) GFP intensity in the QC of 88 strains of WOX5GFP/*atsk21/22/23* lines (45 strains of W5-1 line plus 43 strains of W5-2 line); of 82 strains of WOX5m3DGFP/*atsk21/22/23* lines (40 strains of 3D-1 line plus 42 strains of 3D-2 line); and of 80 strains of WOX5m5DGFP/*atsk21/22/23* lines (40 strains of 5D-1 line plus 40 strains of 5D-2 line).
(K) PAr of QC at 5DAG of 88 strains of WOX5GFP/*atsk21/22/23* lines (45 strains of W5-1 line plus 43 strains of W5-2 line); of 82 strains of WOX5m3DGFP/*atsk21/22/23* lines (40 strains of 3D-1 line plus 42 strains of 3D-2 line); and of 80 strains of WOX5m5DGFP/*atsk21/22/23* lines (40 strains of 5D-1 line plus 40 strains of 5D-2 line).
(L) PAe of QC at the mature embryonic stage of 61 strains of WOX5GFP/*atsk21/22/23* lines (30 strains of W5-1 line plus 31 strains of W5-2 line); of 65 strains of WOX5m3DGFP/*atsk21/22/23* lines (32 strains of 3D-1 line plus 33 strains of 3D-2 line); and of 64 strains of WOX5m5DGFP/*atsk21/22/23* lines (32 strains of 5D-1 line plus 32 strains of 5D-2 line).
(M~O) mPS-PI staining images of (M) WOX5GFP/*atsk21/22/23* line (PAe = 0.661); (N) WOX5m3DGFP/*atsk21/22/23* line (PAe = 0.062) and WOX5m5DGFP/*atsk21/22/23* line (PAe = 0.047).
Student t test indicates statistical difference, bar = 10 μm, yellow arrows show the QC cells or the cell plates of QC cells.

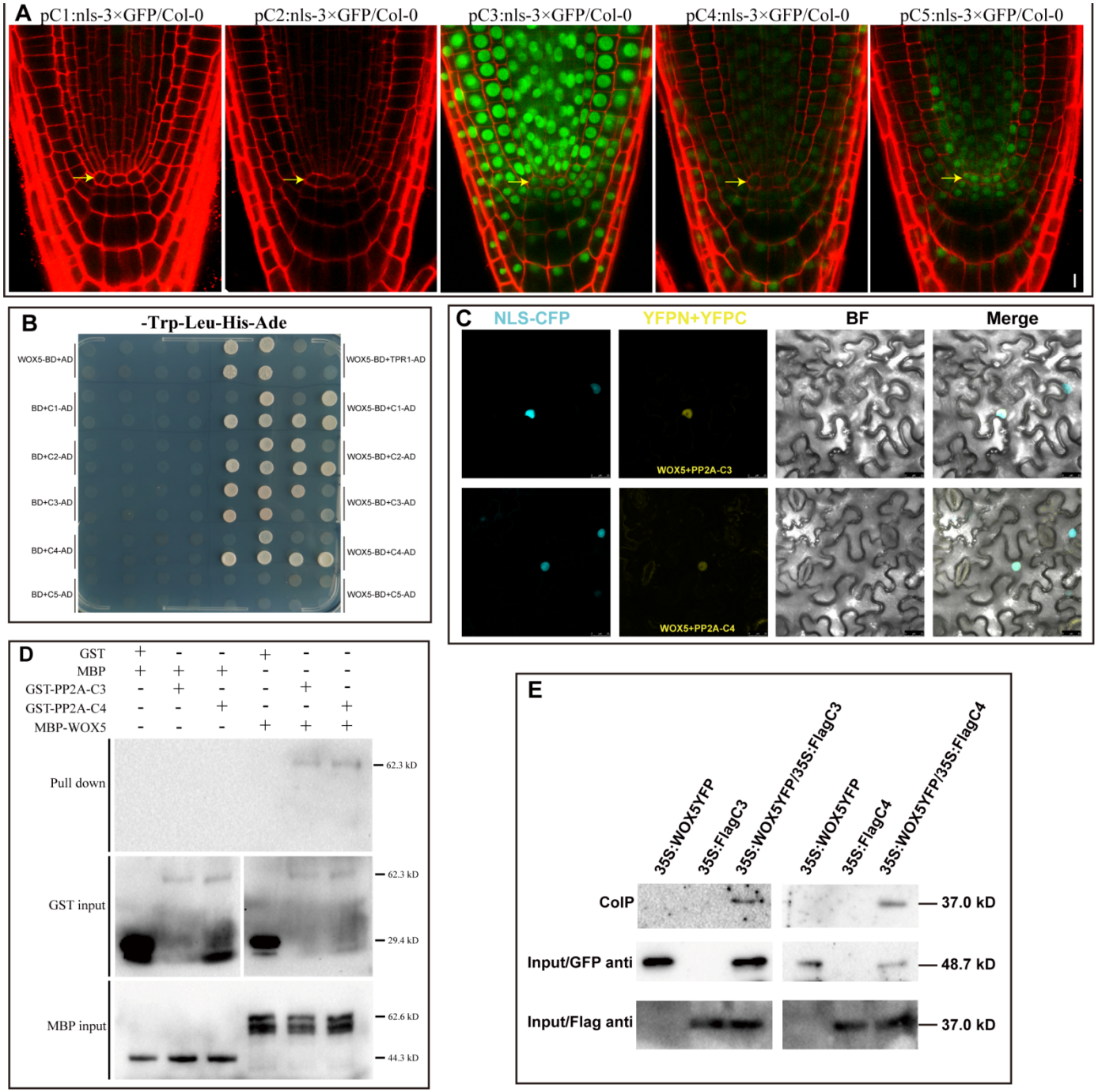

Figure 5: The subfamily II of AtSKs (AtSK21, AtSK22, AtSK23) interact with WOX5 in vitro and in vivo.

Figure 5: The subfamily II of AtSKs (AtSK21, AtSK22, AtSK23) interact with WOX5 in vitro and in vivo.

(A) Transcriptional reporters of the subfamily II of AtPP2A-Cs (AtPP2A-C3, and AtPP2A-C4) and AtPP2A-C5 expressed in the QC at 5DAG.
(B) BiFC assay: NLS-CFP is a nuclear marker, YFPN+YFPC means WOX5-YFPN interacted with AtPP2A-C3-YFPC and AtPP2A-C4-YFPC in nucleus in *the nicotiana tabacum*, , BF is bright filed.
(C) Y2H assay: In the Yeast Base Medium without Trp, Leu, His and Ade, the AH109 strain of positive control group TPR1-BD + WOX5-AD halfly grew (4/8); experiment groups AtPP2A-C1-BD + WOX5-AD and AtPP2A-C1-BD + WOX5-AD mostly grew (6/8), experiment groups AtPP2A-C3-BD + WOX5-AD and AtPP2A-C4-BD + WOX5-AD mostly grew (5/8), but experiment groups AtPP2A-C5-BD + WOX5-AD not grew (0/8).
(D) Pull down in vitro assay: MBP input means MBP protein (44.3 kD) and MBP-WOX5 protein (62.6 kD) exist in the transfer membrane presenting by MBP mouse anti; GST input means GST protein (29.4 kD) and GST-AtSK21 (69.7 kD) exist in the transfer membrane presenting by GST mouse anti; Pull down means only when MBP-WOX5 protein and GST-AtPP2A-C3 or GST-AtPP2A-C4 protein both exist in reaction solution, the GST-AtPP2A-C3 (62.6 kD) or GST-AtPP2A-C4 protein (62.3 kD) could be pull down by MBP beads.
(E) CoIP assay: 35S:WOX5YFP is 35S : LhGR-pOp : WOX5-YFP/Col-0 line, 35S:FlagC3 and 35S:FlagC4 are 35S : FlagAtPP2A-C3/Col-0 line and 35S : FlagAtPP2A-C4/Col-0 line, 35S:WOX5YFP/ 35S:FlagC3 means the double homozygous line of 35S : LhGR-pOp : WOX5-YFP/Col-0 line cross to 35S : FlagC3/Col-0 line, 35S:WOX5YFP/ 35S:FlagC4 means the double homozygous line of 35S : LhGR-pOp : WOX5-YFP/Col-0 line cross to 35S : FlagC4/Col-0 line. Input/GFP anti means WOX5YFP protein (48.7 kD) exist in the transfer membrane presenting by GFP mouse anti, Input/Flag anti means FlagC3 protein (37.0 kD) and FlagC4 protein (36.9 kD) exist in the transfer membrane presenting by Flag mouse anti, CoIP means FlagC3 and FlagC4 protein could be co-immunoprecipitated by GFP beads only in the double homozygous line.
Bar = 10 μm, yellow arrows show the QC cells.

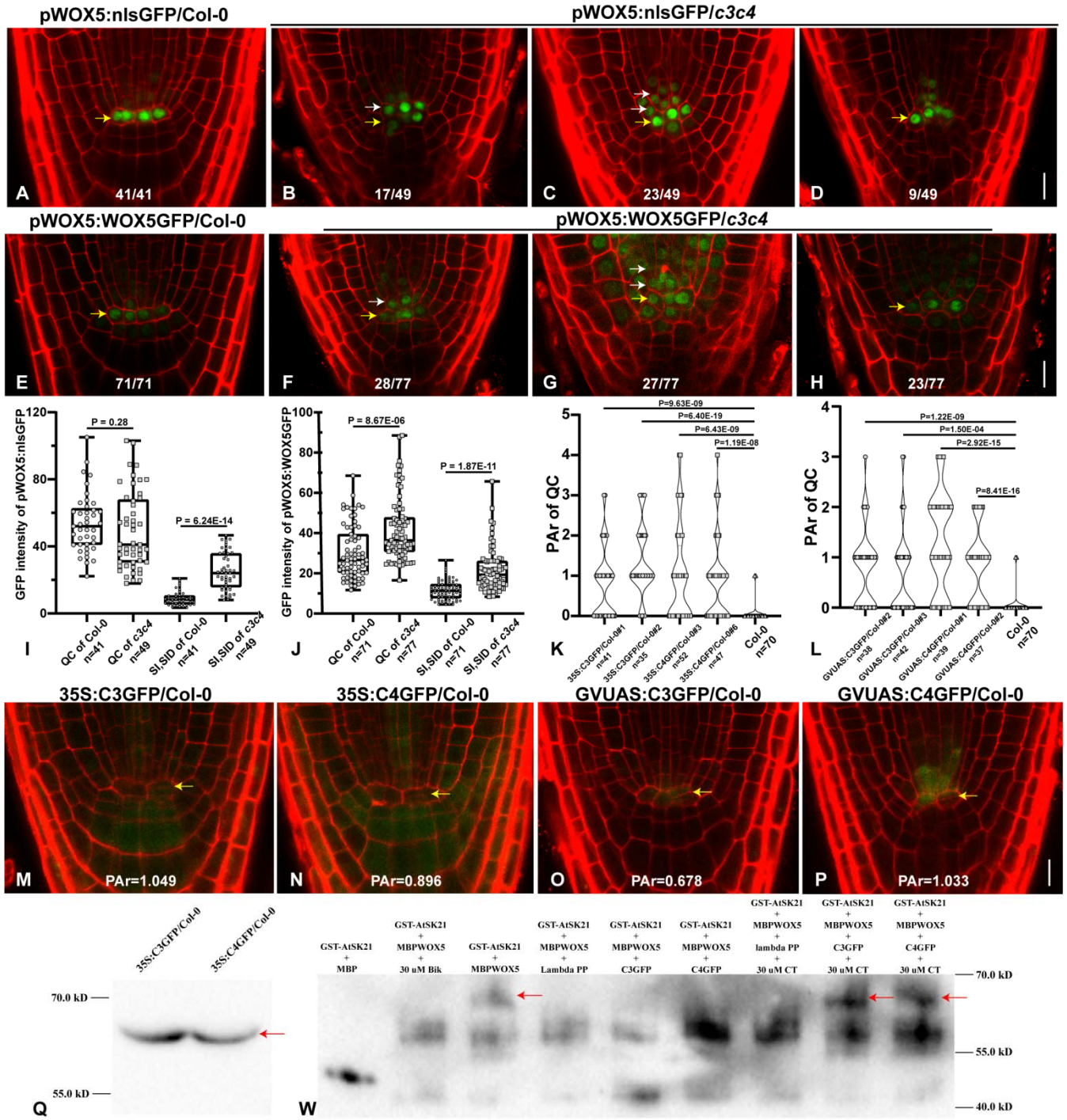

Figure 6:
The subfamily II of AtPP2A-Cs enhance the proliferative activity of QC cells by dephosphorylating and destabilizing the WOX5 protein.

Figure 6: The subfamily II of AtPP2A-Cs enhance the proliferative activity of QC cells by dephosphorylating and destabilizing the WOX5 protein.

(A~D) PI staining images of (A) pWOX5:nlsGFP/Col-0 and (B~D) pWOX5:nlsGFP/*c3c4*;

(E~H) PI staining images of (E) pWOX5:WOX5GFP/Col-0 line and (F-H) pWOX5:WOX5GFP pWOX5:nlsGFP/*c3c4*;

(I) GFP intensity in the QC, SI and SID at 5DAG of pWOX5:nlsGFP/Col-0 (n=41) and pWOX5:nlsGFP/*c3c4*; (n=49);

(J) GFP intensity in the QC, SI and SID at 5DAG of pWOX5:WOX5GFP/Col-0 (n=71) and pWOX5:WOX5GFP/*c3c4*; (n=77);

PI staining images of (D) pWOX5:WOX5GFP×Ws and (E) pWOX5:WOX5GFP×*atsk21/22/23*;

(K) PAr of QC at 5DAG of 35S:C3GFP/Col-0 line #1 (n=41), 35S:C3GFP/Col-0 line #2 (n=35), 35S:C4GFP/Col-0 line #3 (n=52), 35S:C4GFP/Col-0 line #6 (n=47) and Col-0 (n=70);

(L) PAr of QC at 5DAG of GVUAS:C3GFP/Col-0 line #2 (n=38), GVUAS:C3GFP/Col-0 line #3 (n=42), GVUAS:C4GFP/Col-0 line #1 (n=39), GVUAS:C4GFP/Col-0 line #2 (n=37) and Col-0 (n=70);

(M~P) PI staining images of (M) 35S:C3GFP/Col-0 line (PAr = 1.049); (N) 35S:C4GFP/Col-0 line (PAr = 0.896); (O) GVUAS:C3GFP/Col-0 line (PAr = 0.678) and (P) GVUAS:C4GFP/Col-0 line (PAr=1.033).

(Q) C3GFP (63.3 kD) and C4GFP (63.2 kD) fused protein are immunoprecipitated by GFP beads and presented by GFP mouse anti from the 35S:C3GFP and 35S:C4GFP lines.

(W) The Mn2+-Phos-tag™ SDS-PAGE assay, from the left to the right, the first lane showed the negative control (NC) group 1 (GST-AtSK21 + MBP), the second lane showed NC group 2 (GST-AtSK21 + MBP-WOX5 + 30 μM Bik), the third lane showed the experiment group 1 (GST-AtSK21 + MBP-WOX5) with a band (the red arrow) bigger than the MBP-WOX5 band, the fourth lane showed the experiment group 2 [GST-AtSK21 + MBP-WOX5 + lambda Protein Phosphase (PP)], the fivth lane showed the experiment group 3 (GST-AtSK21 + MBP-WOX5 + C3GFP holoenzyme), the sixth lane showed the experiment group 4 (GST-AtSK21 + MBP-WOX5 + C4GFP holoenzyme), the seventh lane showed the experiment group 5 (GST-AtSK21 + MBP-WOX5 + lambda PP + 30 μM CT), the eighth lane showed the experiment group 6 (GST-AtSK21 + MBP-WOX5 + C3GFP holoenzyme + 30 μM CT) with a band (the red arrow) bigger than the MBP-WOX5 band, and the ninth lane showed the experiment group 7 (GST-AtSK21 + MBP-WOX5 + C4GFP holoenzyme + 30 μM CT) with a band (the red arrow) bigger than the MBP-WOX5 band.

Yellow arrows show the QC or the cell plates of QC cells, white arrows show the QC-like cells; Student t test indicates statistical difference, bar = 10 μm.

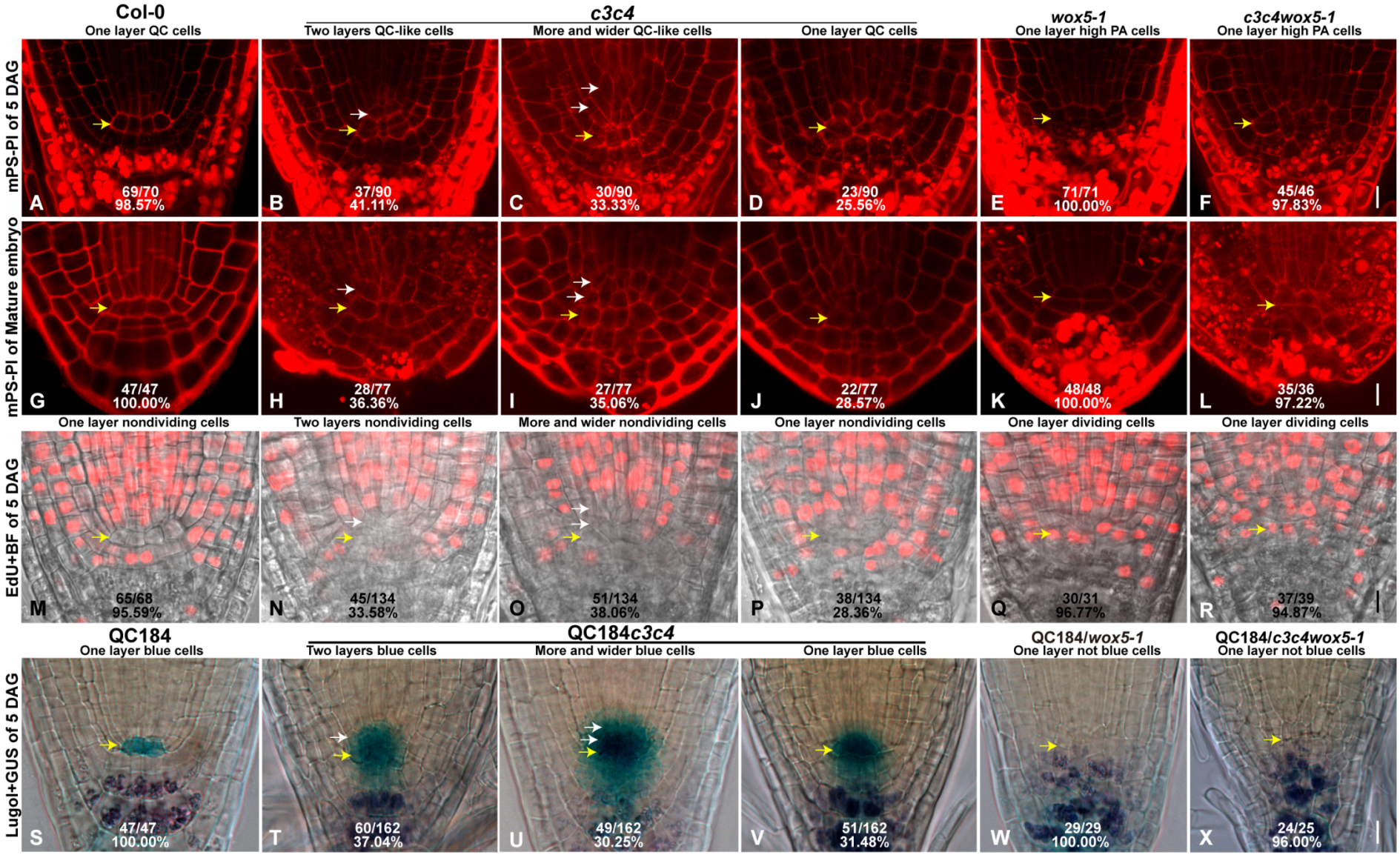

Figure 7:

WOX5 is necessary for producing more quiescent cells when loss of function the subfamily II of AtPP2A-Cs.

Figure 7: WOX5 is necessary for producing more quiescent cells when loss of function the subfamily II of AtPP2A-Cs.

(A~F) mPS-PI staining images of 5DAG of (A) Col-0 (98.57% are one layer QC cells); (B~D) *c3c4* (41.11% are two layers QC-like cells, 33.33% are more and wider QC-like cells, 25.56% are one layer QC cells); (E) *wox5-1* (100.00% are one layer high PA cells); (F) *c3c4wox5-1* (97.83% are one layer high PA cells), yellow arrows show the QC cells, white arrows show the QC-like cells.
(G~L) mPS-PI staining images of mature embryo of (G) Col-0 (100.00% are one layer QC cells); (H~J) *c3c4* (36.36% are two layers QC-like cells, 35.07% are more and wider QC-like cells, 28.57% are one layer QC cells); (K) *wox5-1* (95.59% are one layer high PA cells); (L) *c3c4wox5-1* (97.22% are one layer high PA cells), yellow arrows show the QC cells, white arrows show the QC-like cells.
(M~R) EdU staining and bright filed images of 5DAG of (M) Col-0 (98.57% are one layer nondividing cells); (N~P) *c3c4* (33.58% are two layers nondividing cells, 38.06% are more and wider nondividing cells, 28.36% are one layer nondividing cells); (Q) *wox5-1* (96.77% are one layer dividing cells); (R) *c3c4wox5-1* (94.87% are one layer dividing cells), yellow arrows show the dividing or nondividing cells, white arrows show the QC-like cells.
(S~X) GUS staining images of 5DAG of (S) QC184 (100.00% are one layer blue cells); (T~V) QC184*c3c4* (37.04% are two layers blue cells, 30.25% are more and wider blue cells, 31.48% are one layer blue cells); (Q) QC184/*wox5-1* (100.00% are one layer not blue cells); (R) QC184/*c3c4wox5-1* (96.00% are one layer not blue cells), yellow arrows show the not blue or blue cells, white arrows show the QC-like cells.
Bar = 10 μm.